Design of Magnetic Coordination Polymers Built from Polyoxalamide Ligands: A Thirty Year Story

Yves Journaux, Jesús Ferrando-Soria, Emilio Pardo, Rafael Ruiz-Garcia, Miguel Julve, Francesc Lloret, Joan Cano, Yanling Li, Laurent Lisnard, Pei Yu, et al.

Design of Magnetic Coordination Polymers Built from Polyoxalamide Ligands, a Thirty Years Story

Yves Journaux[a*], Jesús Ferrando-Soria[b], Emilio Pardo[b], Rafael Ruiz-Garcia[b], Miguel Julve[b], Francesc Lloret[b], Joan Cano[b], Yanling Li[a], Laurent Lisnard[a], Pei Yu[c], Humberto Stumpf[d] Cynthia L. M. Pereira[d]

[a] *Sorbonne Universités UPMC Univ Paris 06, CNRS UMR 8232, Institut Parisien de Chimie Moléculaire, Paris, France*
[b] *Instituto de Ciencia Molecular (ICMol)/Departament de Química Inorgànica, C/Catedrático José Beltrán 2, Universitat de València, 46980 Paterna (València), Spain*
[c] *Université Paris Sud, Institut de Chimie Moléculaire et des Matériaux d'Orsay, UMR 8182, F-91405 Orsay, France*
[d] *Departamento de Química, ICEX, Universidade Federal de Minas Gerais, Av. Antônio Carlos, 6627, Belo Horizonte, MG 31270-901, Brazil*

E-mail :yves.journaux@upmc.fr

Web site : http://www.ipcm.fr/JOURNAUX-Yves

Incipit

For this thematic issue dedicated to the attractive legacy of Oliver Kahn, we decided to write this paper on magnetic coordination polymers built from a polyoxalamide ligands. Some of the authors of this paper were part of the exciting adventure at the time of the creation of the Kahn's group at the University of Paris-Sud. Kahn's credo was to synthesize magnetic compounds with predictable structure and magnetic properties and in order to achieve this goal one needs some backgrounds in physics, theory and synthetic chemistry. We have therefore tried throughout this contribution to describe the historical process and the approach of the group's behind the choice of oxamate and oxamidate ligands to synthesize hetero-metallic coordination polymers.

Introduction

It is legitimate to ask the question why bother with magnetic coordination polymers (MCPs). First of all for the synthetic challenge, it is not an easy task to organize magnetic ions or molecules in nD (n =1,2,3) networks. This is still a hot subject as confirmed by the impressive number of articles devoted to molecular-programmed self-assembly,

crystal engineering and metal-organic frameworks (MOFs). Secondly the preparation of molecule-based magnets (MBMs) that requires at least the interaction between the magnetic centers in two dimensions. This topic started at the end of the eighties aiming at obtaining magnets with interesting properties like transparency or low density and furthermore tunable by organic chemistry and easily synthesizable at low temperatures under soft chemistry conditions[1–3]. More recently the discovery of Glauber's dynamics in 1D CPs[4] has renewed the interest in the synthesis of this type of compounds to obtain Single Chain Magnets (SCMs). For both MBMs or SCMs systems it is compulsory to gather a large number of strongly interacting magnetic centers. Some background in physics and in the theory of exchange interaction associated to a synthetic strategy are essential in order to achieve this goal.

A Hint of Physics

In the early time of MBMs story, the choice of synthesizing 1D MCPs to obtain MBMs was dictated by the chemistry but not by the physics. It was already well established that the possibility of magnetic ordering is related to the magnetic anisotropy and dimensionality of the network as shown in Table 1.[5]

Table 1. Magnetic ordering versus dimensionality of the network and magnetic anisotropy

	Ising	XY	Heisenberg
1D	No	No	No
2D	Yes	KT Transition	No
3D	Yes	Yes	Yes

Apart isotropic systems (Heisenberg model) it is possible to have an easy plane (XY model) or an easy axis (Ising model) of magnetization. There is no magnetic ordering for purely 1D systems whatever the anisotropy is. Actually the argument for the 1D Ising model is easy to understand. The flipping of magnetic moments at one specific place that destroys the ordered moments to create domains of different orientations costs only J in energy but this flipping could be made at an infinite number of places and this brings a huge entropy term which decrease the free energy except at $T = 0$ (eqn (1)).

$$\Delta G = \Delta E - T\Delta S = J - T\,k\,\log[\Omega] \qquad (1)$$

Consequently, a disordered system is thermodynamically favored

Magnetic ordering with $M \neq 0$ for 2D networks is only obtained for the Ising model. In the case of the XY model, there is a Kosterlitz-Thouless transition at finite temperature from vortex-antivortex pairs organization at low temperature to free vortex above the transition temperature.[6] However, the overall magnetization remains zero below the transition temperature. Finally, there is no magnetic ordering for the Heisenberg model in 2D networks.

In fact, only 3D networks can present a magnetic ordering for all models and obviously this is the right target to obtain MBMs.

Another important point to have in mind when envisaging MBMs is the connectivity of the network. In the mean field approximation, the Curie temperature (T_C) for a ferrimagnet with two kinds of magnetic centers is given by eqn (2)

$$T_C = \frac{J_{AB}}{3\,k_B}\sqrt{Z_A.S_A(S_A+1)Z_B.S_B(S_B+1)} \qquad (2)$$

where J_{AB} is the interaction between the spins S_A and S_B and Z_A and Z_B are the number of neighbors for A and B respectively. All the involved parameters (magnitude of the interaction, spin size and number of neighbors) have to be as large as possible in order to get high ordering temperatures. Therefore, the choice made by Kahn's group consisting of using a mononuclear copper(II) complex with spin S_{Cu} = =1/2 and connectivity 2 as one component of the ferrimagnetic network was not optimal and had to be compensate by high values of the interaction and spin size for the second magnetic ion.

The interest of physicists in low-dimensional systems is at the origin of Table 1. Originally, the mathematical difficulties to solve the Heisenberg Hamiltonian in three dimensions (3D) was the motivation for theoretical physicists to devote many efforts on low-dimensional physics using simple models like the Ising one[7]. In spite of these simplifications, only the Ising model in one and two dimensions was exactly solved. The resolution of the 2D model by Onsager[8] is still considered as a mathematical tour de force. Recently, it was shown that the Ising model is computationally intractable in 3D[9]. Nevertheless, these theoretical works bring out some interesting predictions about the physics of low dimensional magnetic systems. In particular Glauber predicted in 1963 slow relaxation of magnetization in ferromagnetic Ising chains[10] but at that time there was no good 1D ising system to check this prevision. The discovery in 2001 of slow relaxation in a ferrimagnetic Co-radical coordination polymer [4,11] was the confirmation of the Glauber's prediction. As noted by Caneschi *et al*[11] the reason of this late verification is due to the two strict conditions needed to observe this phenomenon: (i) Ising-type anisotropy and (ii) a very high *J/J'* ratio, between the intra- and interchain exchange interactions which preclude any magnetic ordering before very low temperatures. Molecule-based compounds are particularly adapted to fulfill the second

condition owing to the presence of ligands that can be specially designed to decrease the interchain interaction.

Theory

Until the mid-seventies, the Anderson's model[12] and the Goodenough-Kanamori[13–15] rules (GK) were the only theoretical guides to understand and predict the nature of interaction between magnetic ions. Actually if one does not look at the details of the calculations, the Anderson's theory looks counterintuitive to molecular chemists. For instance, the singlet-triplet energy gap in a dicopper(II) complex is given by eqn (3)

$$\Delta E = 2K_{a,b} - \frac{4\,t_{a,b}^2}{U} \qquad (3)$$

where $K_{a,b}$ is the bielectronic exchange integral ($K_{a,b} =< a(1)b(2)\left|{}^{1}/_{r_{12}}\right|a(2)b(1) >$) always positive, $t_{i,j}$ the transfer integral $t_{a,b} =< a|\hat{h}|b>$ ($\hat{h}$ being the monoelectronic hamiltonian) and U the energy of the metal-metal charge transfer configuration (MMCT). The antiferromagnetic interaction comes from the interaction between the ground state and the MMCT configuration where one ion is a copper(I) and the other a copper(III). This is obviously a very high energy excited state if one takes into account the generally observed coordination sphere of the copper ions making unlikely the actual existence of such a mechanism. In a very interesting paper, Weihe *et al* have shown that the value od U is not the energy of the MMCT configuration but an effective value strongly reduced by hybridization effects.[16] They also have shown that calculations using reasonable value for all the integrals and in particular for U, do not lead when using the Anderson's formula to value of ΔE close to the experimental one. Furthermore it is puzzling that in the Anderson's theory, the most important component of the interaction appears at the second order in perturbation indicating that there is something behind the scenes. It is the reason why the publication in mid-seventies of the Kahn's [17–19] and Hay, Thibeault and Hoffmann's models[20] was of tremendous importance for molecular magnetism. Both of them relate the value of the interaction to concepts familiar to chemists or to computable parameters. In particular, the antiferromagnetic interaction in the Kahn's model appears at first order in perturbation and it highlights the key role of the overlap between the magnetic orbitals. The single-triplet energy gap in a dinuclear copper(II) complex for this model is given by eqn (4).

$$\Delta E = 2K_{a,b} + 4\,t_{a,b}\,S_{a,b} \qquad (4)$$

Where $t_{a,b} =< a|\hat{h}|b>$ and $S_{a,b}=<a|b>$ are the one-electron transfer and overlap integrals respectively, As they are of opposite sign, their product favors the antiferromagnetic coupling. The antiferromagnetic component for the Hay's model appears at the second order but could be evaluated from the calculation of the energy gap between the symmetric and antisymmetric MOs build from the magnetic orbitals [eqn (5)]

$$\Delta E = 2K_{a,b} + \frac{(e_1 - e_2)^2}{J_{ab} - J_{aa}} \quad (5)$$

where e_1 and e_2 are the energies of the symmetric and antisymmetric MOs built from the magnetic orbitals and J_{aa} and J_{ab} are the mono- and bicentric Coulomb integrals respectively. The difference between the two models is due to the nature of the wave functions basis set, natural magnetic orbitals and localized orthogonal magnetic orbitals for Kahn's and Hay's models, respectively. It should be noted that Anderson also used localized orthogonal Wannier wave functions[12] and this explains why the antiferromagnetic component appears at the second order in Anderson's and Hay's models. The driving forces for the ferro- and antiferromagnetic couplings in the Kahn's model are very clear: antiferromagnetic interaction is obtained when there is a net overlap between the magnetic orbitals and on the contrary, a ferromagnetic coupling is observed when these orbitals are orthogonal by symmetry or accidentally. In general, the antiferromagnetic component largely overcomes the ferromagnetic one. It is worthy of note that the role of the overlap and orthogonality between the magnetic orbitals was already highlighted by Anderson when he gave in 1963 his own formulation of the Goodenough Kanamori's rules in a book chapter « Exchange Interaction in Insulators »[21].

Rule A : *« When the two ions have lobes of magnetic orbitals pointing toward each other in such a way that the orbitals would have a reasonably overlap integral, the exchange is antiferromagnetic. »*

Rule B : *« When the orbitals are arranged in such a way that they are expected to be in contact but to have no overlap integral- most notably a d($3z^2$-r^2) and d(xy) in 180° position, where the overlap is zero by symmetry, the rule gives ferromagnetic interaction (not, however, usually as strong as the antiferromagnetic one) »*

Interestingly, this formulation of the Goodenough Kanamori rules was unknown in the mid-seventies by many of magnetochemists including O. Kahn (personal communication). In general, chemists involved in the field of magnetism use the original formulation of the Goodengouh Kanamori's rules.[13,14] However they are not well adapted for molecular magnetism where in most of the cases the actual geometry is far from the ideal case described in the Goodenough Kanamori's rules. For instance, there are unable to predict the magneto-structural correlation between the nature and magnitude of the magnetic coupling with the Cu–O–Cu bridging angle (Φ) for a series of ferro- and antiferromagnetically coupled di-μ-hydroxodicopper(II) complexes (J = 7.27 x 10^3 –74.53Φ) published in 1976 by Hatfield *et al*.[22] The Goodenough Kanamori's rules are also useless in the case of polyatomic bridges such as oxalate. For all these reasons, the publication of the Kahn's model has been a milestone in molecular magnetism. In fact, it has paved the way for the rational design and synthesis of exchange-coupled,

homo- and heterodinuclear complexes with predictable magnetic properties. The importance of his theoretical work was reinforced by the synthesis by Kahn and coworkers of textbook examples illustrating his model. He show that it is possible to obtain strong magnetic interactions either ferro- or antiferromagnetic in complexes where the magnetic orbitals are orthogonal by symmetry or having a net overlap, respectively[23,24] A scheme of the heterodinuclear complex [CuVO(bfsaen)(MeOH)] [H_4bfsaen = *N,N'*-bis(2-hydroxy-3-carboxybenzylidene)-1,2-diaminoethane] where the magnetic orbital are orthogonal by symmetry, the triplet ground state being stabilized by 118 cm^{-1} with respect to the excited singlet state (Figure 1), is the cover picture of the Kahn's reference book « *Molecular Magnetism* ».[25] It is amazing that this textbook example of symmetry imposed ferromagnetic interaction is close to the sub-rule (c) of rule A given by Anderson « *(this is not actually a case discussed in these terms by any authors mentioned but we feel it follows logically from the same principles) In a 90° ligand situation, when one ion has a d($3z^2$-r^2) occupied and the other a d(xy), the pπ for one is the pσ for the other and one expect strong overlap and thus antiferromagnetic exchange ».* Anderson is undoubtedly right for a mono-bridged situation but considering double bridged situation and replacing *d(3z2-r2)* by *d(x2-y2)*, the rule can be reformulate to state the opposite conclusion « *In a 90° ligand situation for double-bridged compound , when one ion has d(x2-y2) occupied and the other a d(xy), the pπ for one is the pσ for the other and one expect zero overlap and thus ferromagnetic exchange ».* All this is to say that it is important to consider the whole symmetry, an incorrect conclusion could be reached if the analysis is made bridge by bridge.

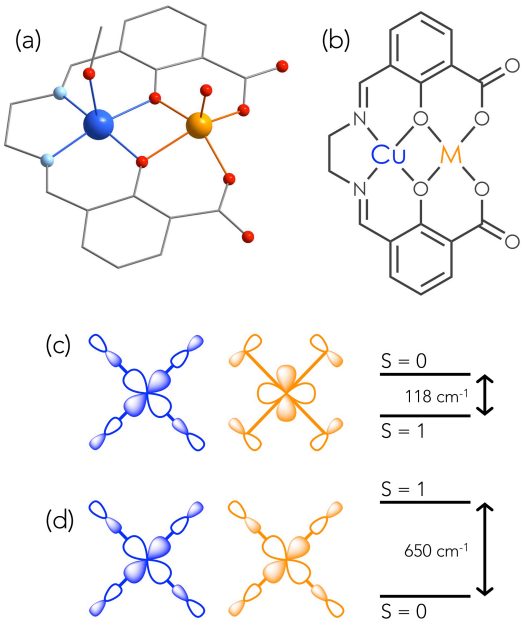

Figure 1. Molecular structure of [CuVO(bfsaen)(MeOH)] (a) and general chemical structure of [CuM(bfsaen)(MeOH)] (M = VO, Cu) (b) showing the pair of magnetic orbitals and energy of the states for the bis(phenoxo)-bridged copper(II)-vanadium(IV) (c) and dicopper(II) (d) complexes.

Kahn and co-workers have also shown that it is possible in some way to control the overlap between the magnetic orbitals by means of the orbital reversal strategy induced by nitrogen containing ligands (Figure 2) and therefore to tune the antiferromagnetic interaction in dinuclear complexes[26,27] as well as in CPs.[28]

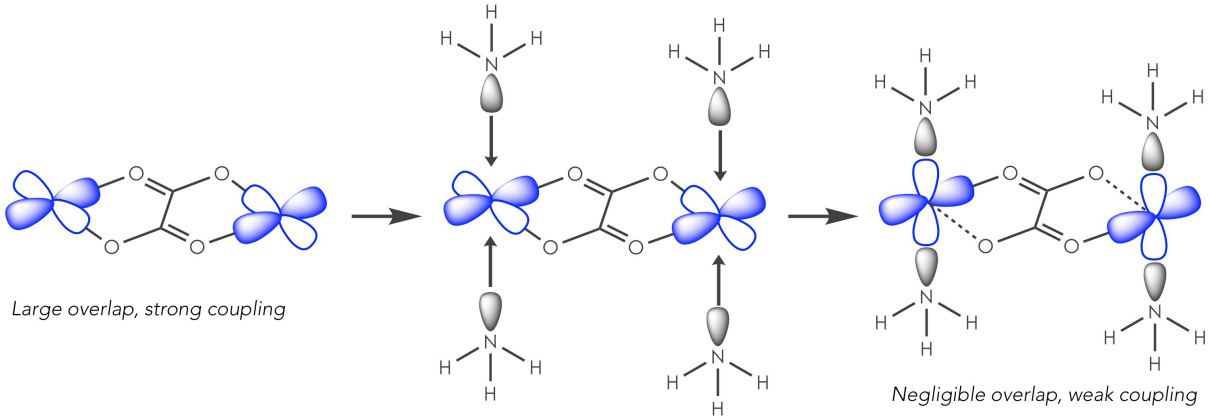

Figure 2. An illustration of orbital reversal phenomenon: orientation of the magnetic orbitals in $Cu(C_2O_4)\cdot 1/3H_2O$ and $Cu(C_2O_4)(NH_3)_2\cdot 2H_2O$.

Hay's and Kahn's models allow to understand why the overwhelming majority of compounds presents antiferromagnetic interaction due to the overlap between the magnetic orbitals and tell us that ferromagnetic interaction is generally relatively weak and obtained only under very peculiar conditions. So, although at first sight ferromagnetic interaction seems to be the right target to obtain MBMs or SCMs it is not the best approach to obtain magnetic ordering (MBMs) or slow relaxation of magnetization (SCMs) at reasonable temperatures. Consequently, ferrimagnetic compounds are the best alternative to obtain SCMs or MBMs because the strategy they represent takes advantage of a generally strong AF coupling and this type interaction is the easiest to obtain in practice. This is the reason why the Kahn's group chose this strategy in the eighties to obtain MCPS and MBMs.

What about the Ligand ?

The problem was to find a good bridging ligand able to transmit electronic interactions and giving also an easy access to heterometallic compounds in order to obtain ferromagnetic CPs. The choice of the complex-as-ligand strategy (metalloligand) seems very appropriate because it allows the stabilization of a first magnetic ion in a known environment and the presence of donor atoms makes possible the coordination of a second magnetic ion. After the initial attempts with the symmetric oxalate ligand[29] that only fulfill the first condition and a first success with the synthesis of heterobimetallic chains using the dithioxalate bridging ligands[30] it was obvious that dissymmetric ligands are the key ingredient to the success; otherwise, it is necessary to play with the reaction kinetics and use metalloligands synthesized with inert metal ions. In this

context, the possible choice of bridging ligands becomes limited. The oximato bridge is one possibility and actually the magnetic coupling between copper(II) ions through this bridge is extremely large (ca. -700 cm^{-1}).[31,32] However, as far as we know, no single crystal of MCPs has been obtained[33,34]. Cyanide is also an obvious choice but it was not considered in the Orsay period by the Kahn's group for no reason and its incredible success to synthesize MCPs[35–39] and room temperature MBMs[40–44] arrived later in the nineties. At that time oxamate and oxamidate ligands looked like the good choice. They are dissymmetric ligands that afford a priori easy access to heterometallic compounds[45], also being able to mediate electronic interaction as large as –440 cm^{-1}[27]. But besides these favorable characteristics, one of the main advantages of oxamate and oxamidate ligands deals with the possibility to change the substituent on the nitrogen atom allowing the tuning of the steric effects or providing a way to improve the solubility in different solvents, introducing other coordinating groups or even additional functions such as chirality, redox activity, conductivity and luminescent properties, etc. A selection of oxamic acid derivatives to be used as ligands after deprotonation is depicted in Figure 3.

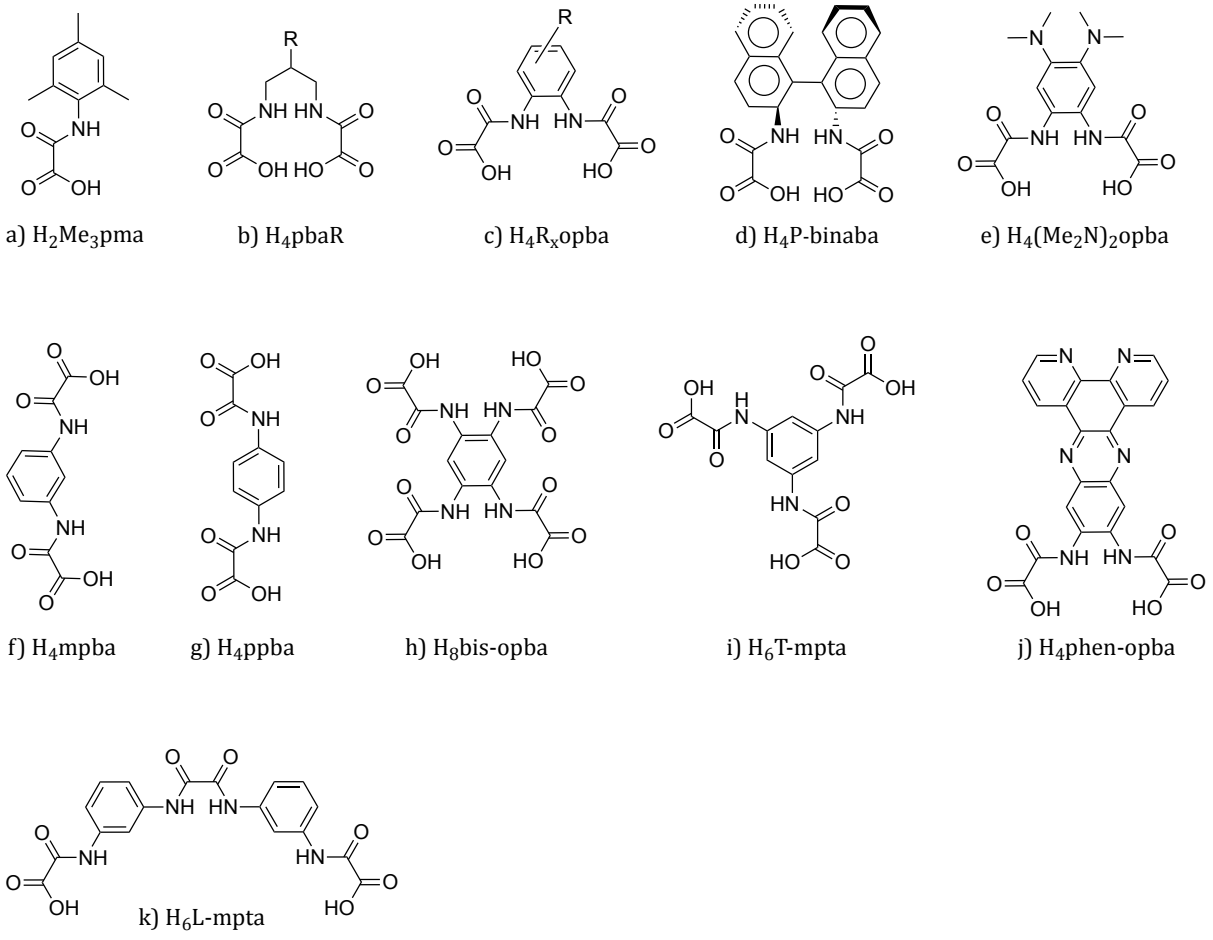

a) H_2Me_3pma b) H_4pbaR c) H_4R_xopba d) H_4P-binaba e) $H_4(Me_2N)_2opba$

f) H_4mpba g) H_4ppba h) H_8bis-opba i) H_6T-mpta j) H_4phen-opba

k) H_6L-mpta

Figure 3. Some oxamic acid derivatives: (a) bidentate, (b,c) tetradentate, (d) chiral, (e) redox active, (f,g)

bis-bidentate, (h,k) tris-bidentate, (i) bis-tetradente, (j) ditopique

For all these reasons, Yu and Journaux started to work with oxamate and oxamidate ligands in the Kahn's group in the eighties with two main targets: heterometallic complexes[46–48] and MCPs[49] and specially MBMs[2]. Coordination of two oxamate ligands to a copper(II) ion through the deprotonated amidate-nitrogen and carboxylate-oxygen atoms leads to a very stable dianionic complex that can act as a bis-bidentate ligand through its free oxygen atoms towards either fully solvated metal ions or preformed complexes bearing labile ligands in their coordination sphere. To further increase the stability of the dianionic monometallic copper(II) complex, Yu used tetradentate ligands containing two oxamate groups. In general, the pro-ligand as ethyl ester derivative is used as starting material instead of the corresponding oxamic acid derivative (Figure 4, top). Recently, *N*-substituted phenyloxamate ligands have been employed because the phenyl groups usually adopt a *trans* arrangement in the copper(II) metalloligand, a feature that allows a better control of the possible intermolecular interactions.

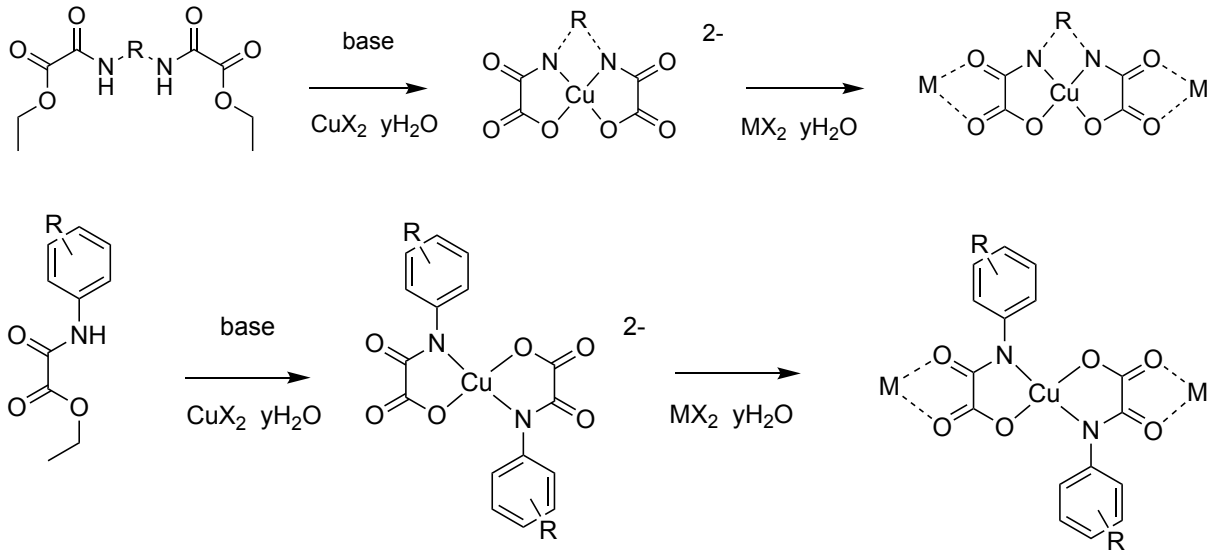

Figure 4. Schematic view of the preparative route of 1D CPs of general formula $\{[CuL_x]M(solv)_2\}_n$ (L = oxamate ligand, x = 1 or 2, M = Cu, Mn, Co or Ni and solv = H_2O, DMSO or DMF).

These mononuclear copper(II) precursors are linear connectors perfectly adapted to synthetize 1D CPs (Figure 4). Moreover, as dianonic metal complexes they are able to react with divalent metal ions to form highly insoluble heterobimetallic neutral chains. This preparative route has allowed the synthesis of a great number of 1D MCPs.

1D coordination polymers (CPs)

Molecule-Based Magnets (MBMs)

Strong interchain interactions are required to obtain MBMs with 1D CPs. In the mean field approximation, the critical ordering temperature (T_C) for Heisenberg ferromagnetic chains is given by eqn (6)[50]

$$T_C = \frac{S(S+1)}{k}\sqrt{J_{intra} \cdot J_{inter}} \qquad (6)$$

where S is the local spin value, and J_{intra} and J_{inter} are the intra- and interchain interactions, respectively. The use by Yu Pei of non bulky bis(oxamate) ligands with alkyl chains [see Figure 4] afforded the first example of an oxamate-containing MBM (R = $CH_2CHOHCH_2$)[2] The hydroxyl group was introduced on purpose to favor hydrogen bonding between the neighboring chains as depicted in Figure 5.

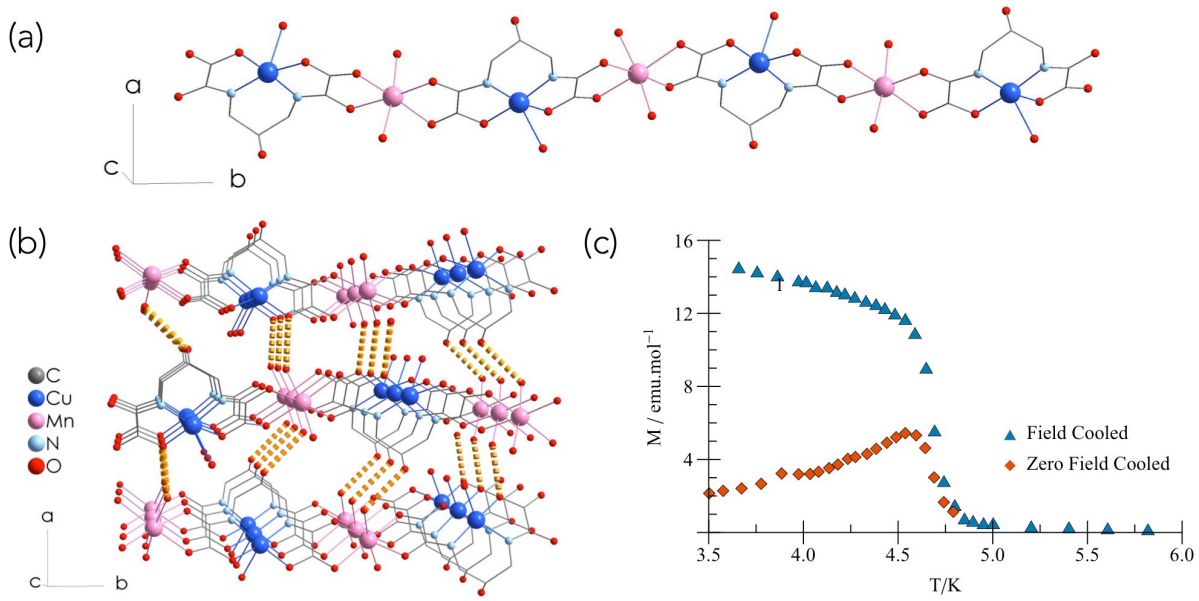

Figure 5. (a) View of a fragment of the chain structure of $[MnCu(pbaOH)(H_2O)_3]_n$. (b) Perspective view of the hydrogen bonds linking the chains along the crystallographic *c* axis. (c) Temperature dependence of the magnetization (*M*) for the heterobimetallic chain in the temperature range 6-3.5 K and under a dc field of 3 x 10^{-2} G.

In addition to this role, the hydroxy group shifts the chains to each other along the crystallographic *b* axis and it causes the shortest interchain Mn(II)···Cu(II) separation (ca. 5.751 Å) in the *a* direction. This arrangement is reminiscent of the idea put forward by McConnell as early as 1963 to get ferromagnetic interactions between organic radicals[51]. The overall ferromagnetic coupling between the ferrimagnetic chains occurs through the interaction between strong positive spin densities located on the manganese(II) ions belonging to one of the chains and weak negative spin densities on the copper(II) ions from the neighboring chain (Figure 6).

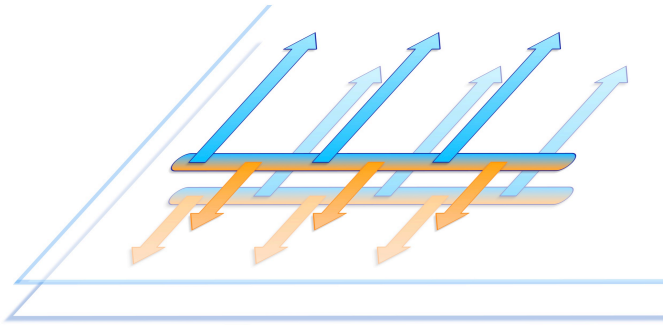

Figure 6. Schematic view of the ideal arrangement of chains leading to interchain ferromagnetic interactions through the McConnell's mechanism.

As a consequence, $[MnCu(pbaOH)(H_2O)_3]_n$ (**1D-MnCu-pbaOH-a**) chain presents a magnetic ordering at Tc = 4.6 K as shown in Figure 5c. Nevertheless, in spite of this success, this approach is rather limited due to the lack of the total control of the packing of the chains in the crystal making impossible to warrant interchain ferromagnetic interactions. This is welll illustrated by the existence of an another phase obtained with the same pbaOH ligand $[MnCu(pbaOH)(H_2O)_3{\cdot}2(H_2O)]_n$ (**1D-MnCu-pbaOH-b**) [52] where the shortest interchain metal-metal separation involve metal ions of the same type. In such a case, the main interchain magnetic interaction implies the same kind of spin density and consequently, according to McConnell's mechanism, an antiferromagnetic ordering is observed at T_N = 2.3 K. Furthermore, in spite of the hydrogen bonding network, the interchain interaction remains weak precluding a high temperature magnetic ordering. The fortuitous discovery that vacuum treatment affects dramatically the magnetic properties an oxamidate-bridged Cu(II)Mn(II) CPs moving from an antiferromagnetic compound at 2.3 K to a ferromagnetic one at 14 K[53,54] moved us to try vacuum and heat treatment on the oxamato-based 1D MCPs. In particular, warming **1D-MnCu-pbaOH-a** chain in the solid phase at 100 °C under vacuum for 48 h afforded a new species of formula $MnCu(pbaOH)(H_20)$ (**1D-MnCu-pbaOH-c**)[55]. The magnetic properties of this new compound are not affected down to 50 K showing that the intrachain interaction is not modified by the heat treatment. On the other hand, the magnetic properties for T < 50 K are deeply modified to finally exhibit a ferromagnetic transition at Tc = 30 K as shown in Figure 7.

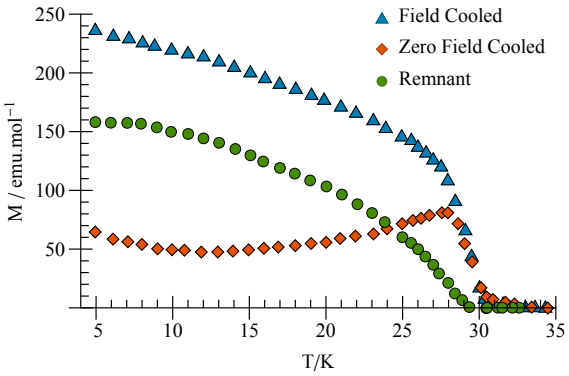

Figure 7. Temperature dependence of the magnetization (*M*) for **1D-MnCu-pbaOH-c** in the 5-35 K temperature range and a field of $3x10^{-2}$ Oe.

The coordinated and crystallization solvent molecules are removed by the vacuum and heat treatment inducing a solid state cross-linking that increases the interchain interactions allowing a higher ordering temperature as inferred from eqn (6). Although this strategy has been very effective, the cross-linking process is far from being controlled and it does not allow the synthesis of MBMs by design. As seen in Table 1 the right solution to obtain MBMs by a rational design consists of increasing the dimensionality of the network.

Single Chain Magnets (SCMs)

By contrast, oxamidate-based 1D CPs perfectly match the materialization of SCMs. The possibility to change the substituent on the nitrogen atom allows the rational design of bulky oxamidate-containing ligands that are able to induce a very high J/J' quotient between the intra- (J) and interchain (J') exchange interactions avoiding any magnetic ordering prior to very low temperatures. This is one of the two strong requirements in order to observe slow relaxation of the magnetization in 1D compounds. In this respect, the tetradentate ligands used by the Kahn's group during the Orsay period are not the best candidates to obtain SCMs. The bulky part of the ligand in the mononuclear copper(II) metalloligand is only at one side and this allows relative close contacts between the neighboring chains on the other side. Actually, even if there is no magnetic ordering in the Cu(II)Co(II) chains within the opba family of ligands [Figure 3c], none of these chains present SCM behavior. The six-coordinate cobalt(II) ions bring the Ising-type anisotropy which is the second important condition to obtain SCM behavior.

As mentioned above, the *N*-substituted phenyloxamate ligands are more appropriate to synthesize SCMs given that the two bidentate ligands L generally adopt a *trans* conformation in the starting mononuclear $[CuL_2]^{2-}$ building block which creates steric hindrance on both sides of the copper(II) metalloligand. However, this structural feature creates steric hindrance only in the same plane as the oxamate group. To really isolate the chain in the third direction, it is necessary to rotate the phenyl rings perpendicular

to the oxamate group. This conformation is obtained when there are substituents at the *ortho* position of the amide function as shown in Figure 8. The presence of substituents on the phenyl rings also favors the *trans* arrangement of the oxamate ligands in the copper(II) complex in order to avoid steric hindrance between substituents of the two coordinated oxamate ligands [Figure 8b].

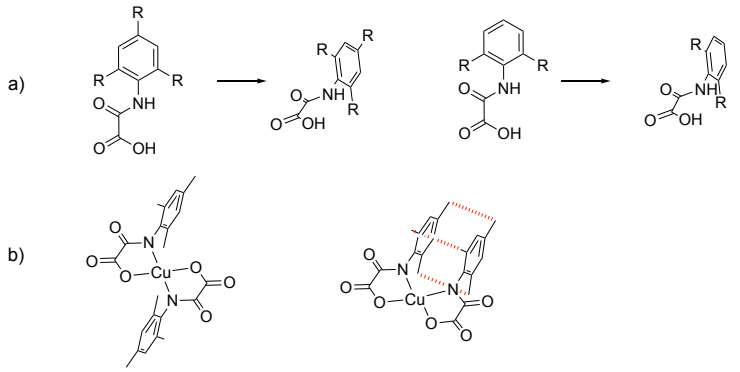

Figure 8. Schematic 3D views of (a) *N*-substituted phenyloxamate ligands showing the rotation of the aromatic ring and (b) bis(oxamato)cuprate(II) complexes in *trans* and *cis* conformations showing the steric hindrance for the *cis*-conformation (the red dashed lines represent the possible steric hindrances).

Heterobimetallic chains of general formula $[MCu(Me_xpma)_2(H_2O)_y(DMSO)_z]_n$ were obtained with (Me_2pma) = *N*-2,6-dimethylphenyloxamate and (Me_3pma) = 2,4,6-trimethylphenyloxamate.[56,57] The X-ray structures of two of these Cu(II)Co(II) 1D systems were solved, namely $[CoCu(Me_2pma)_2(H_2O)_2]_n$ (**1D-CoCu-Me$_2$pma**) and $\{[CoCu(Me_3pma)_2(H_2O)_2]\cdot 4H_2O\}_n$ (**1D-CoCu-Me$_3$pma**). Both compounds consist of neutral oxamato-bridged cobalt(II)–copper(II) chains. The two water molecules coordinated to the cobalt(II) ion in first chain are in a *cis* arrangement leading to a zig-zag chain as depicted in Figure 9a. Because of the *cis* conformation of the six-coordinate cobalt(II) ions, two different isomers (Δ and Λ) exist that alternate regularly along the chain. The chains are rather well separated from each other, the shortest interchain Co···Co and Cu···Co distances being 5.995(5) and 6.628(3) Å, respectively. The fact that the phenyl rings are practically perpendicular to the oxamate groups causes an effective shielding between the neighboring chains. However, there are weak interchain hydrogen bonds interactions involving the coordinated water molecules and the carbonyl oxygen atoms of the oxamate ligands (Figure 9b).

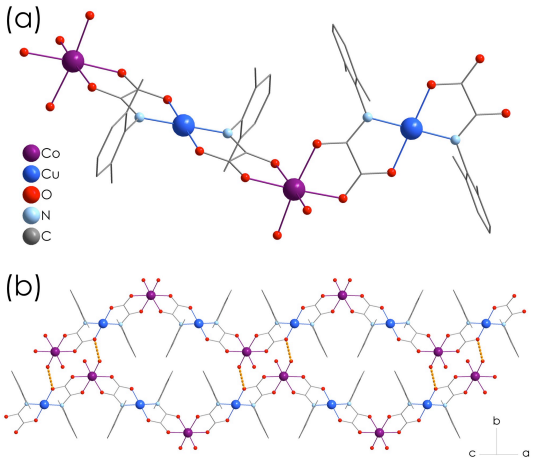

Figure 9. (a) View of a fragment of the **1D-CoCu-Me$_2$pma** chain with the atom labeling for the coordination environment of the metal ions. Hydrogen atoms are omitted for clarity. (b) Crystal packing of the chains along the [101] direction. Hydrogen bonds are represented by dashed lines [symmetry code: (a) =1/2-*x*, ½-*y*, -*z*; (b) = -*x*, *y*, ½-*z*; (c) = *x*, 1-*y*, 1-*z*; (d) = *x*, *y*, ½-*z*].

The two water molecules coordinated to the cobalt(II) ion in the second chain are in *trans* positions leading to a ribbon-like chain as depicted in Figure 10a. The phenyl rings are practically perpendicular to the oxamate groups generating an effective shielding between the adjacent chains. This leads to well separated chains (Figure 10b), the shortest interchain metal–metal separation being 8.702(3) Å [Co···Co and Cu···Cu; Figure 10b). There are, however, some weak interchain hydrogen bonds along the crystallographic *b* axis involving the coordinated and the crystallization water molecules which result into a supramolecular square motif (Figure 10c).

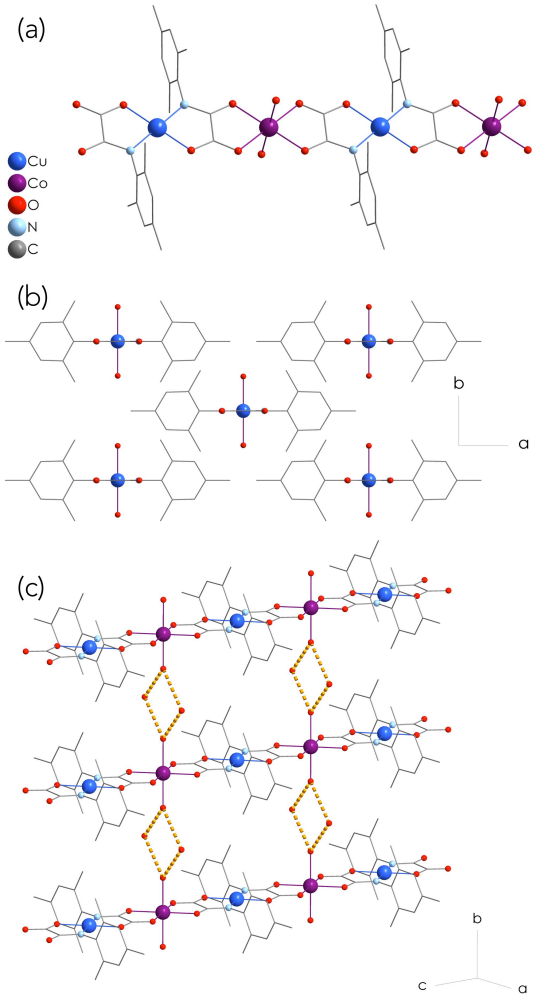

Figure 10. (a) View of a fragment of the **1D-CoCu-Me$_3$pma** chain with the atom labeling for the metal coordination environments (hydrogen atoms are omitted for clarity). (b) and c) Crystal packing of the chains along the [001] and [111] directions. Hydrogen bonds are represented by dashed lines [symmetry code: (a) = -*x*, *y*, -*z*; (b) = -*x*, *y*, 1-*z*; (c) = *x*, 1+*y*, *z*; (d) = 1+*x*, *y*, *z*; (e) =1/2-*x*, ½-*y*, -*z*].

The dc magnetic behavior under the form of $\chi_M T$ versus T plot of these compounds are characteristic of ferrimagnetic chains with the presence of a minimum around 100 K. The intrachain interaction between the Co(II) and Cu(II) ions is quite large with J_{CoCu}= -45.8 cm^{-1} and 35.0 cm^{-1} for **1D-CoCu-Me$_2$pma** and **1D-CoCu-Me$_3$pma**, respectively. The ac magnetic properties of these cobalt(II)–copper(II) chains show evidence of slow magnetic relaxation effects which are typical of SCMs. χ_M'' becomes nonzero below 3.0 K for **1D-CoCu-Me$_2$pma**, but no χ_M'' maxima are observed above 2.0 K. Therefore, it is not possible to determine the dynamic of the relaxation process for this chain. On the other hand, χ_M'' show a frequency-dependent maxima between 2.3 K (1400 Hz) and 2.0 K (300 Hz) for **1D-CoCu-Me$_3$pma** (Figure 11b). The calculated values of τ at T_{max} follow the Arrhenius law characteristic of a thermally activated mechanism [$\tau = \tau_0 \exp(E_a/k_BT)$] (Figure 11a, inset). The values of the activation energy (E_a) and pre-exponential factor (τ_0) are 16.3 cm^{-1} and 4.0 x 10^{-9} s, respectively.

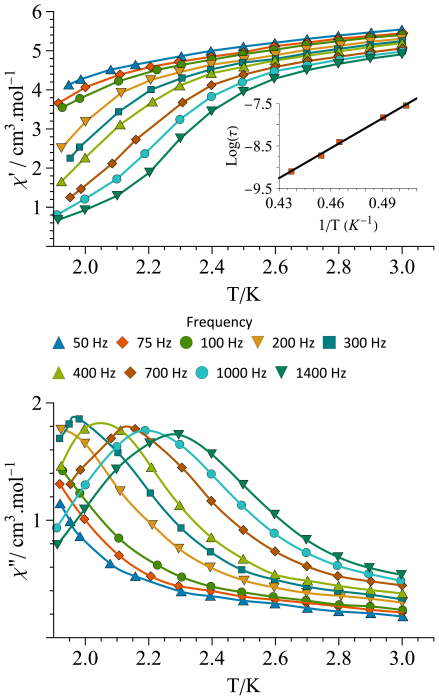

Figure 11. Temperature dependence of (a) χ_M' and (b) χ_M" of **1D-CoCu-Me$_3$pma** in zero applied static field and under 1 Oe oscillating field at different frequencies of the oscillating field. The solid lines are eye-guides. The insets show the Arrhenius plot (see text).

The design of sterically hindered aromatically substituted oxamate ligands has allowed the synthesis of well isolated Cu(II)Co(II) neutral chains with a very high J/J' ratio between the intra- and interchain interactions thereby fulfilling the condition to observe properties of slow relaxation of the magnetization. All the members of this family of compounds except the monosubstituted ligand show evidence of slow relaxation[57]. These results shows the huge advantage of oxamate ligands linked to the possibility to modify the substituent of the nitrogen atom of the oxamate function in order to introduce steric hindrance but also other properties such as chirality.

In this respect, Pardo *et al*, were able to synthesize chiral heterobimetallic chains[58,59]. The strategy is based on the use of enantiopure chiral sterically-hindered dianionic bis(oxamato)cuprate(II) complexes with the enantiomerically pure (*M*)-1,1'-binaphthalene-2,2'-bis(oxamate) [(*M*)-binaba] and (*P*)-1,1'-binaphthalene-2,2'-bis(oxamate) [(*P*)-binaba] ligands (Figure 12).

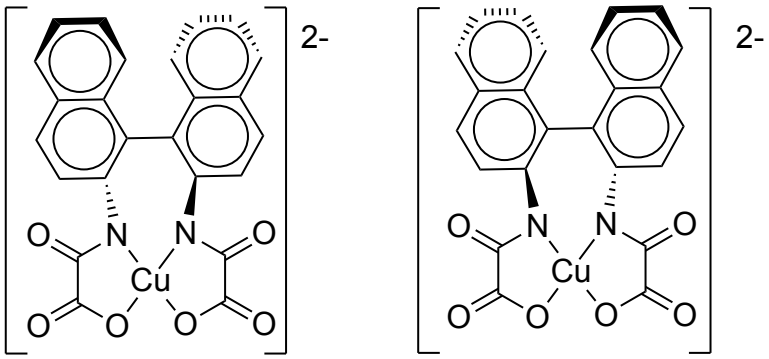

Figure 12 . Schematic view of [*M*-Cu(*M*)-binaba]$^{2-}$ and [*P*-Cu(*P*)-binaba]$^{2-}$.

Such complexes act as bis(bidentate) ligands towards fully solvated cobalt(II) ions. These enantiopure copper(II) precursors transfer their chiral information to the stereochemistries of the Co(II) metal centers in a controlled manner. The enantiopure {[Co(Λ)-Cu(*M*)-binaba(DMF)$_2$]DMF}$_n$ (**1D-Λ-CoCu-M-binaba**) and {[Co(Δ)-Cu(*P*)-binaba(DMF)$_2$]DMF}$_n$ (**1D-Δ-CoCu-P-binaba**) helicoidal chains are obtained with the [*M*-Cu(*M*)-binaba]$^{2-}$ and [P-Cu(P)-binaba]$^{2-}$ metalloligands respectively, as depicted in Figure 13. The coordination sphere of the cobalt(II) ions are completed by two DMF molecules in *cis* positions.

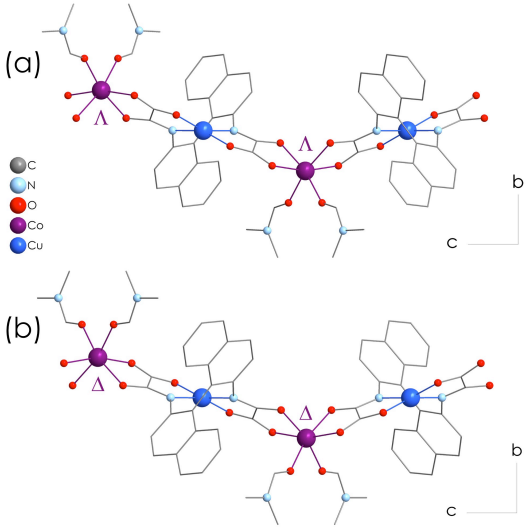

Figure 13 . Views of fragments of the (a) **1D-Λ-CoCu-M-binaba** and (b) (**1D-Δ-CoCu-P-binaba**) chains with the atom labeling of the metal coordination environments. Hydrogen atoms have been omitted for clarity [symmetry code: (c) = x+1, y, z+1/2].

The binaba ligands are bulkier than the Me$_x$pma ligands and the coordinated DMF molecules contribute also to an effective shielding between neighboring chains. The shortest interchain Co···Co and Co···Cu distances being 9.3233(15) and 9.1947(12) Å for **1D-Λ-CoCu-M-binaba** and 9.5239(15) and 9.2827(11) Å for **1D-Δ-CoCu-P-binaba**. Consequently, the alternating current (ac) magnetic properties of the enantiopure cobalt(II)–copper(II) chains showed evidence of slow magnetic relaxation effects, χ_M'' being frequency-dependent below 4.0 K for both compounds (Figure 14). The ac

magnetic properties of **1D-Λ-CoCu-M-binaba** were studied at very low temperature in order to investigate the dynamic properties of this chain.

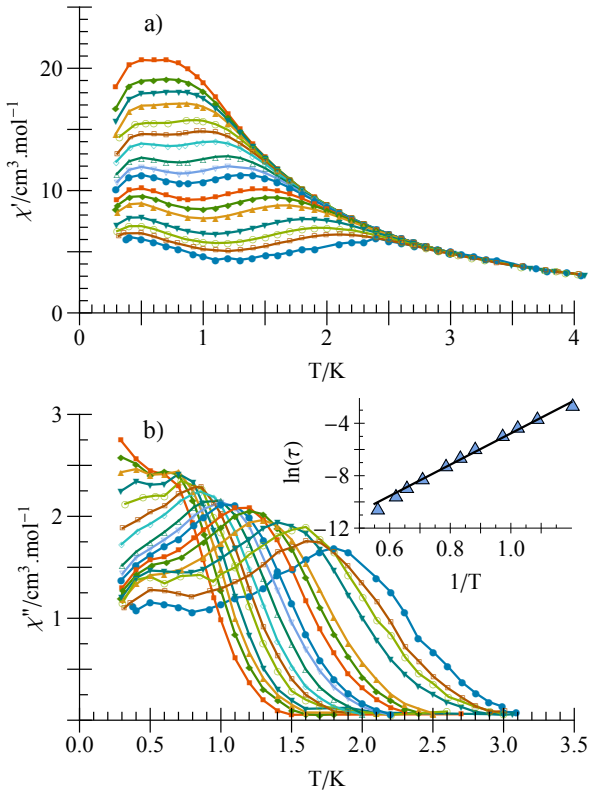

Figure 14. Temperature dependence of the (a) in-phase and b) out-of-phase magnetic susceptibilities of **1D-Λ-CoCu-M-binaba** under zero applied static field at different frequencies (0.021–5700 Hz) of the 1 G oscillating field. The inset shows the Arrhenius plot.

A second frequency-independent peak in the ac susceptibility is observed at 0.4 K (Figure 14), which can be attributed to magnetic 3D ordering at these very low temperatures. The calculated values of τ at T_{max} follow the Arrhenius law characteristic of a thermally activated mechanism (inset in Figure 14b) with an energy barrier (*E*a) to reverse the magnetization direction of 9.2 cm^{-1} and a pre-exponential factor (τ_0) of 2.2 x 10^{-8} s. The two chiral chains **1D-Λ-CoCu-M-binaba** and **1D-Δ-CoCu-P-binaba** are the first examples of Chiral Single Chain Magnets. (CSCMs). Furthermore, because of the chiral centers are on the magnetic ions, this ensures a strong coupling between the two properties opening perspectives to observe the magneto-chiral effect in this kind of compounds[60,61] with higher blocking temperatures. This family of compounds are the prototype of multifunctional magnetic materials (MMMs) where the coexistence of two properties generates a third one.

To conclude this part on 1D MCPs, bis(bidentate) oxamate derivatives are perfectly appropriate to design 1D polymers. The presence of alky/aryl substituents on the nitrogen atoms which create steric constraints is likely a handicap for the synthesis of

MBMs because the resulting decrease of the interchain interactions that is required to obtain magnetic ordering. On the other hand, this is an important asset to study one-dimensional physics as it allows to control the steric effects. Moreover, tailor-made substituents allows to develop multifunctional materials associating the magnetism with other physical properties.

2D coordination polymers

As stated in the presentation of 1D CPs, it is necessary to increase the dimensionality of the structures to expect higher ordering temperatures for MBMs and 2D networks constitute the next target even so Ising type anisotropy is needed to observe magnetic ordering. Three connections in the same plane are required to build 2D CPs. First, Journaux *et al* designed tripodal ligands with three oxamidate ligands but had only little success along this line.[62] On the other hand, when looking at the zig-zag chain (Figure 9a), it seems obvious that it is possible to coordinate a third oxamate group instead of solvent molecules on the six-coordinate metal site. The resulting $\{[Cu(II)L]_3M(II)_2\}^{2-}$ network is negatively charged and countercations are required to compensate the charge. In 1993 Stumpf *et al.* explored this strategy by using a weakly coordinating methylpyridinium-nitronylnitroxyde radical cation in order to cross-link the 2D networks and obtain a 3D network which favors the magnetic ordering. The result was polycatenated 2D networks[63] $\{(Me\text{-}rad)_2Mn_2[Cu(opba)l_3(DMS0)_2{\cdot}2H_2O\}n$ (**2D-MnCu-opba-a**)[64]. The polycatenated networks are nearly perpendicular as depicted in Figure 15.

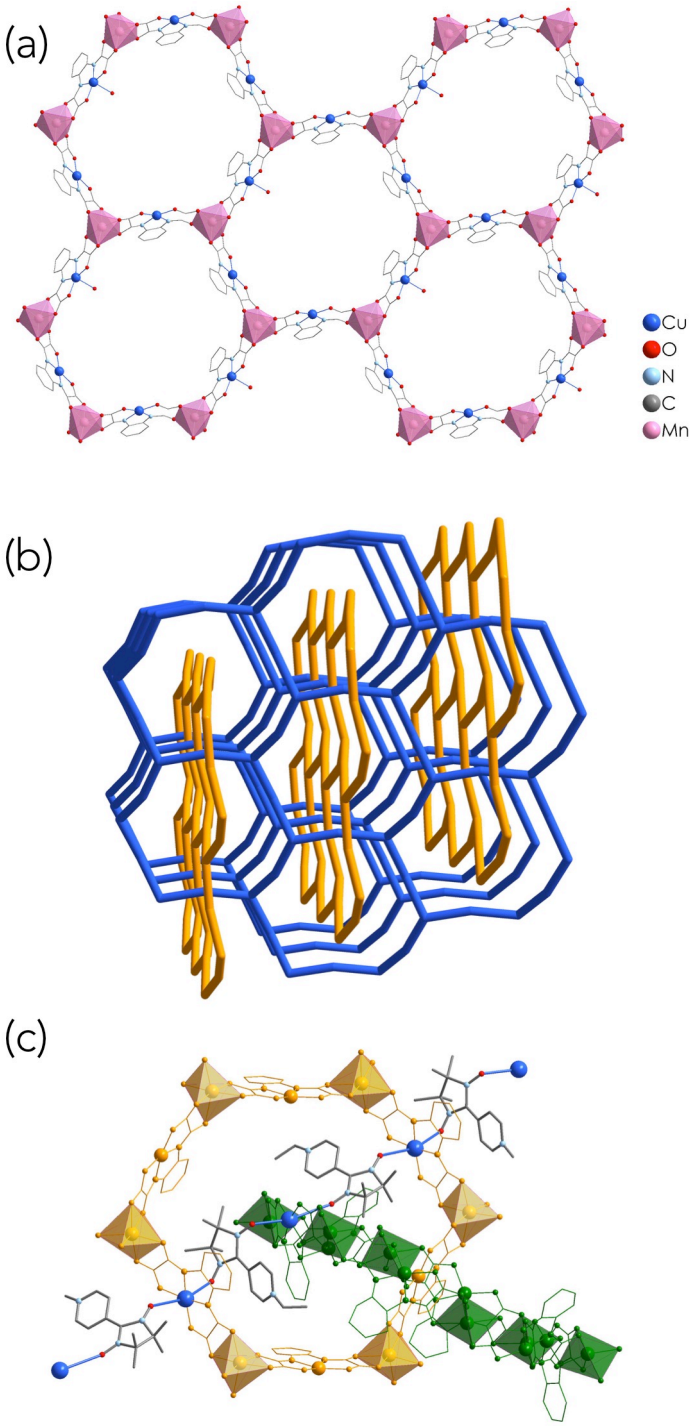

Figure 15. View of **2D-MnCu-opba-a** (a) the 6.3 hexagonal network, (b) the polycatenation of the 6.3 network and (c) the rad-Cu chain that cross-links the polycatenated 6.3 network.

The polycatenated 6.3 networks are linked by methylpyridium nitronylnitroxyde radicals which are weakly coordinated to the copper(II) ions in axial position. However, the Cu-O distance between the copper(II) ions and the oxygen atoms of the radical are in the range 2.8-3.2 Å, values which likely exclude any strong interaction between the

copper(II) ions and radicals. This weak interaction probably dictates the ordering temperature of **2D-MnCu-opba-a** at 22.5 K (Figure 16).

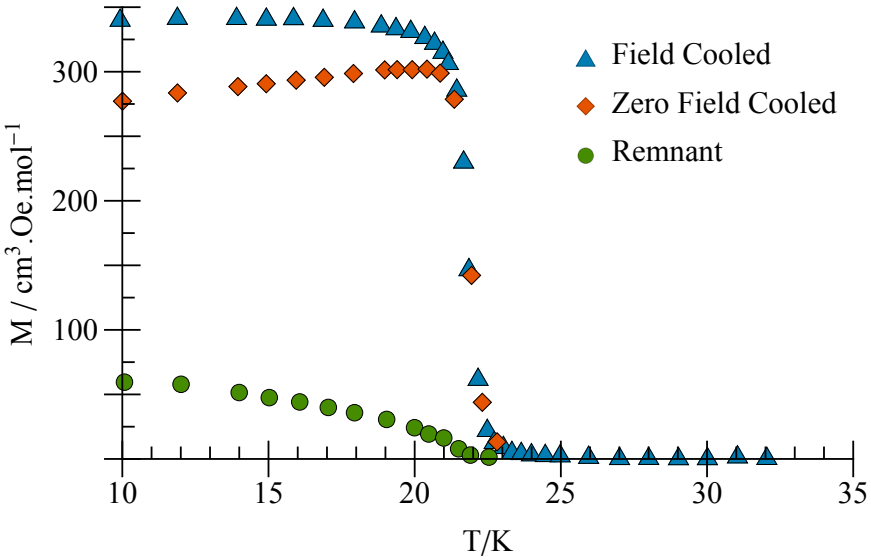

Figure 16. Temperature dependence of the magnetization (*M)* for **2D-MnCu-opba** in the temperature range 10-35 K and under a field of 1 Oe.

Few years later, other polycatenated networks of formula $\{(Et\text{-}rad)_2M_2[Cu(opba)l_3(DMSO)_x(H_2O)_y]_n$ (**2D-MCu-opba-b**) with M = Mn, Co and Ni[65,66] were synthesized by the Kahn's group at Bordeaux with the ethylpyridinium nitronyl-nitroxyde as radical. These compounds are MBMs with magnetic ordering at 22.8, 28 and 37 K for the Mn(II), Ni(II) and Co(II) derivatives, respectively. Interestingly the Ni(II) derivative shows a compensation temperature and a pole inversion.[67,68]

More recently Ferrando-Soria *et al* obtained purely 2D networks using *N*-substituted phenyloxamate ligands. The synthesis is based on the use of the dianionic mononuclear copper(II) complex $[Cu^{II}Me_2pma_2]^{2-}$, where Me_2pma = *N*-2,6-dimethylphenyloxamate as bis-bidentate metalloligand toward the solvated manganese(II) cation. A key point is the use of a large excess of the mononuclear copper(II) precursors (5 : 1 metalloligand to solvated cation molar ratio) in order to prevent the formation of the corresponding 1D compounds discussed above. The structure of $\{(n\text{-}Bu_4N)_4[Mn_4Cu_6(Me_2pma))_{12}(DMSO)_2]\cdot 8DMSO\cdot 2H_2O\}n$ (**2D-MnCu-Me_2pma**) consist of oxamato-bridged $Mn^{II}_2Cu^{II}_3$ bimetallic hexagonal layers of 6_3 or hcb (Reticular Chemistry Structure Resource) which are interleaved by layers formed by the bulky *n*-Bu_4N^+ cations and free water and DMSO molecules[69]. In spite of the presence of chiral Mn^{II} ions coordinated by three bidentate ligands, the structure is achiral due to the

perfect alternation of Λ and Δ isomers in the hexagonal 2D layer as depicted in Figure 17. Actually the regular alternation of Λ and Δ isomers is compulsory to obtain 2D CPs and it has been already verified in the two-fold interpenetred network but also in the oxalate-based heterobimetallic 2D networks.[70,71] The adjacent anionic $Mn^{II}_2Cu^{II}_3$ flat hexagonal layers in the crystal lattice are displaced leading to a staggered stacking in an *ABAB* pattern along the crystallographic *c* axis.

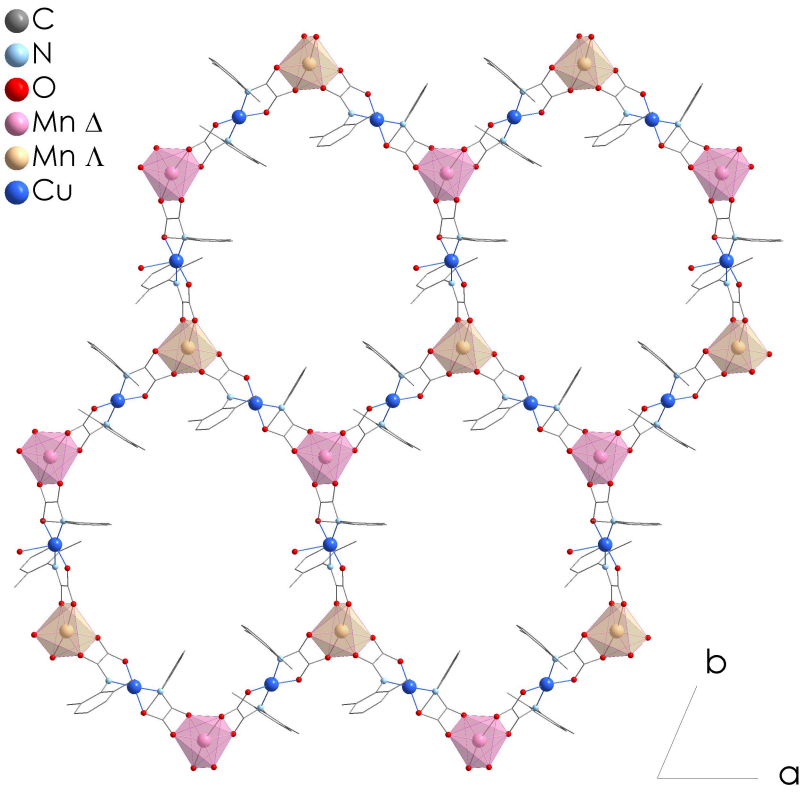

Figure 17. Perspective view of a fragment of $[Mn_4Cu_6(Me_2pma)_{12}(DMSO)_2]^4$ 2D network in the *ab* plane emphasizing the regular alternation of Λ and Δ isomers for the Mn(II) ions. Hydrogen atoms are omitted for clarity

The magnetic properties are typical of ferrigmanets with the presence of a minimum in the $\chi_M.T$ versus T curve at 132 K. The coupling constant between the Cu^{II} and Mn^{II} ions through the oxamate bridge was determined using Quantum Monte-Carlo Calculation and is equal to J = -35.1 cm^{-1}. This compound presents a long-range ferromagnetic ordering at Tc = 10 K. It is not possible to get a magnetic ordering within the 2D network with isotropic ions like Mn(II) (see Table 1). Consequently, the critical temperature is quite low due to the weak interplanar interaction. Unfortunaltely, Ferrando-Soria *et al* were unable to synthesize this 2D network with an Ising type ion like Co(II) which could lead to a magnetic ordering within the plane.

All the previous compounds described in this review have been obtained using dianionic mononuclear copper(II) complexes. However, it is possible to design polyoxamate-containing ligands (APOXAs, Figure 3f-i,k) which consists of a somewhat rigid polymethyl-substituted benzene scaffold with multiple oxamate binding sites of various substitution pattern (polytopic ligands). Starting from mpba and ppba ligands (Figure 3f,g) or polymethyl-substituted derivatives, double-stranded dicopper(II) metallacyclophane precursor complexes $[Cu_2(L)_2]^{4-}$ (L = mpba, Me_3mpba, ppba, Me_4ppba) have been synthesized. These complexes show interesting magnetic properties with a relatively large ferromagnetic coupling for the mpba family where the two oxamate groups are in *meta* position of the phenylene group. The values of *J* are in the range 14-16 cm^{-1} for two copper(II) ions separated by ca. 6.9 Å. By contrast, the ppba familly shows strong antiferromagnetic coupling ($J \approx -90$ cm^{-1}) while the two Cu(II) ions are separated by ca. 7.9 Å. The explanation of these large values for the coupling constant has its origin in the spin-polarisation mechanism (Figure 18).[72–74] In fact, $[Cu_2(Me_x mpba)_2]^{4-}$ (x = 0, 2 and 3) and $[Cu_2(Me_x ppba)_2]^{4-}$ (x = 0,4) are good ferro- and antiferromagnetic coupling units, respectively (FCUs and ACUs).

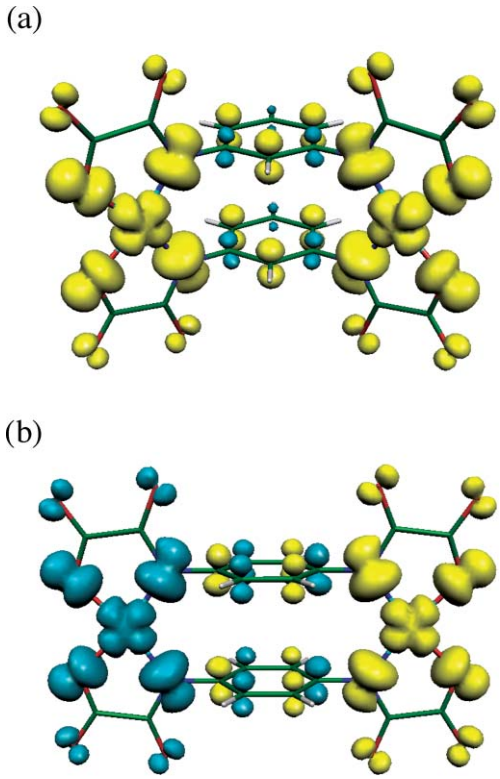

Figure 18. Perspective views of the calculated spin density distribution for the (a) triplet and (b) BS singlet ground spin states in $Na_4[Cu_2(mpba)_2]\cdot 10H_2O$ and $Na_4[Cu_2(ppba)_2]\cdot 11H_2O$, respectively. Yellow and blue contours represent positive and negative spin densities, respectively. The isodensity surface corresponds to a value of 0.0015 e $Å^{-3}$. Reproduced from *Dalton Trans.* **2008**, 2780–2805 with permission from RCS.[75]

This feature allows the control of the magnetic properties of polynuclear complexes or CPs synthesized with these copper(II) complexes as precursors. When these copper(II) building blocks react with salts of M(II) ions [M = Co(II) or Mn(II)] in 1:1 molar ratio, a neutral compound of formula $[M_2Cu_2L_2(H_2O)_x]\cdot yH_2O$ is obtained. The two obvious structures are a ladder-like chain, the rungs being the L ligand, or a brick-wall type structure. The crystal structures of $\{[Co_2Cu_2(mpba)_2(H_2O)_6]\cdot 6H_2O\}_n$ (**2D-CoCu-mpba**) [76] and $\{[Mn_2Cu_2(Me_4ppba)_2(H_2O)_6]\cdot 8H_2O\}_n$ (**2D-MnCu-Me$_4$ppba**)[77] have been solved (Figure 19). Each dicopper(II) metallacyclophane entity acts as a tetrakis(bidentate) ligand through the carbonyl oxygen atoms of the oxamate ligand atoms toward diaquametal(II) units, yielding a brick-wall rectangular layer with a (6,3) net topology. The water molecules coordinated to M(II) ions are in *trans* or *cis* configuration for the **2D-CoCu-mpba** and **2D-MnCu-Me$_4$ppba** compounds respectively. There are six copper atoms within each rectangular cell unit, which occupy the four corners and the middle point of the two long edges of the rectangle, whereas four M(II) ions sit at the one-fourth and three-fourth points of each long edge. Two different isomers (Δ and Λ) alternating regularly along the CuMn chains occur in **2D-MnCu-Me$_4$ppba** because of the *cis* conformation of the octahedral Mn atoms in this compound.

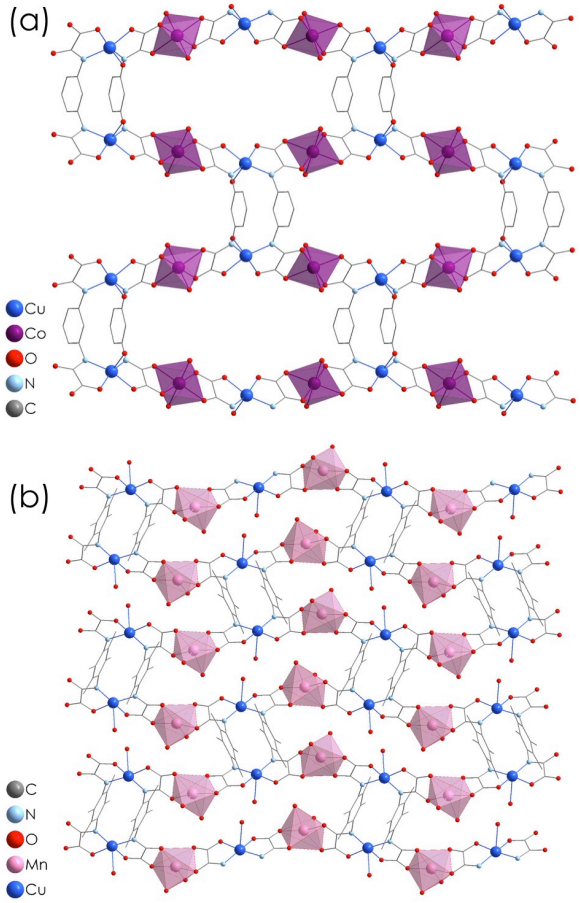

Figure 19 : View of the structure of (a) **2D-CoCu-mpba** and (b) **2D-MnCu-Me$_4$ppba**.

Due to the presence of ACUs in **2D-MnCu-Me$_4$ppba**, the ferrimagnetic $Cu^{II}Mn^{II}$ chains are strongly antiferromagntically coupled and the value $\chi_M T$ at 2.0 K is very low and equal to 0.08 $cm^3 mol^{-1} K$. However, it is worthy of note that there is no maximum of χ_M indicating the lack of AF ordering in this compound as expected for a 2D network containing isotropic ions like Mn(II) (see Table 1). On the other hand, the presence of FCUs in **2D-CoCu-mpba** leads to completely different magnetic properties. The ferrimagnetic $Cu^{II}Co^{II}$ chains are ferromagnetically coupled and the presence of Ising type Co(II) ions should lead to a ferromagnetic transition in the 2D [Cu_2Co_2] plane. However, for measurements made under an applied magnetic field below 1.2 KOe, the magnetization present a maximum which corresponds to a maximum for χ'_M at T_N = 9.5 K in the ac measurements (Figure 20). This is the signature of an antiferromagnetic ordering coming from the weak antiferromagnetic interaction between layers.

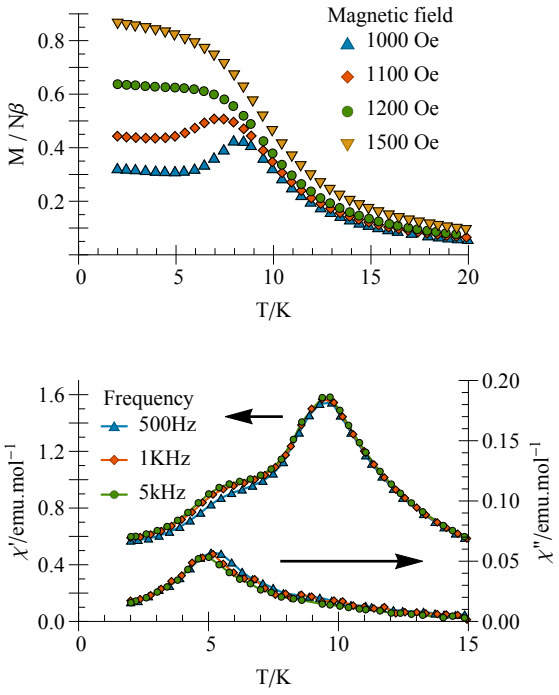

Figure 20 : a) Magnetization (M) versus T for **2D-CoCu-mpba** at 1.0 kOe, 1.1 kOe, 1.2 kOe and 1.5 kOe ; b) χ' and χ'' .

Actually **2D-CoCu-mpba** is a metamagnet and a magnetic field of 1.2 kOe is sufficient to overcome this weak interaction and the compound presents a field-induced transition from an antiferromagnetic to a ferromagnetic-like state. With Me_3mpba ligand, the compound $\{[Co_2Cu_2(Me_3mpba)2(H_2O)_6]\cdot 2H_2O\}_n$ (**2D-CoCu-Me$_3$mpba**) does not show any metamagnetic behavior but it exhibits instead a ferromagnetic ordering at 25 K which is characterized by frequency-independent peaks in χ'_M and χ''_M (see Figure 21)[78]. The crystal structure is unknown but the presence of methyl groups likely changes the packing of the layers and the interlayer interaction do not annihilate the

magnetic ordering within the plane. Interestingly, the Mn(II) derivative with the Me_3mpba ligand $\{[Mn_2Cu_2(Me_3mpba)_2(H_2O)_6]_3 \cdot 8H_2O\}n$ (**2D-MnCu-Me_3mpba**) also shows a ferromagnetic ordering at Tc = 20 K. [77]

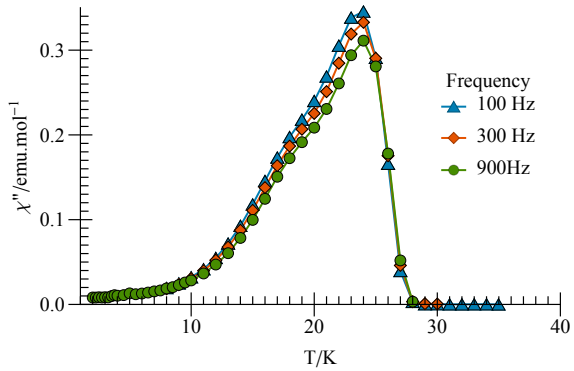

Figure 21. Temperature dependence of out-of-phase magnetic susceptibilities of **2D-CoCu-Me_3mpba**[78].

To conclude this part on 2D CPs, bis-bidentate oxamate ligands or poly bis-bidentate oxamate ligands allow the synthesis of 2D CPs in a controlled way. Some of them are examples of MBMs; however, the occurrence of a ferromagnetic transition strongly depends on the interaction between the 2D networks within the crystal. This interaction is needed in case of isotropic [Cu_xMn_y] networks but it also determines the magnetic properties for very anisotropic 2D networks containing Co(II) ions since possible antiferromagnetic interlayer interactions can result in an antiferromagnetic compound. Unfortunately, in spite of the efficient strategies for synthesizing 2D networks, crystalline engineering knowledge does not allow yet the total control of the stacking of the layers in the crystal, a feature that makes uncertain the synthesis of MBMs. The only way to master the synthesis of MBMs by design is the achievement of 3D networks.

3 connected 3D networks

As shown in the paragraph devoted to the 2D CPs, the use of bis-bidentate ligands such as oxamate leads to nodes with connectivity 3. The possibility of building 3D networks with three connected nodes was approached in 1933 by Laves[79] and extensively studied in 1954 by Wells in his famous series of articles on « The geometrical basis of crystal chemistry »[80]. The construction of 3D networks is obtained by translation without rotation or other symmetry operation of a basic unit in the three directions of space. This basic unit is connected to the others by six links in order to cover all space directions (± x, ±y, ±z). In order to fulfill this requirement, the minimum number of nodes in the basic unit, the so-called Z_t number, is determined by the network connectivity. For instance in six-connected nets only one node is needed and for four

connected nets, two nodes are needed. In the case of three-connected networks, the minimum number of nodes to build a 3D net is equal to four ($Z_t = 4$).

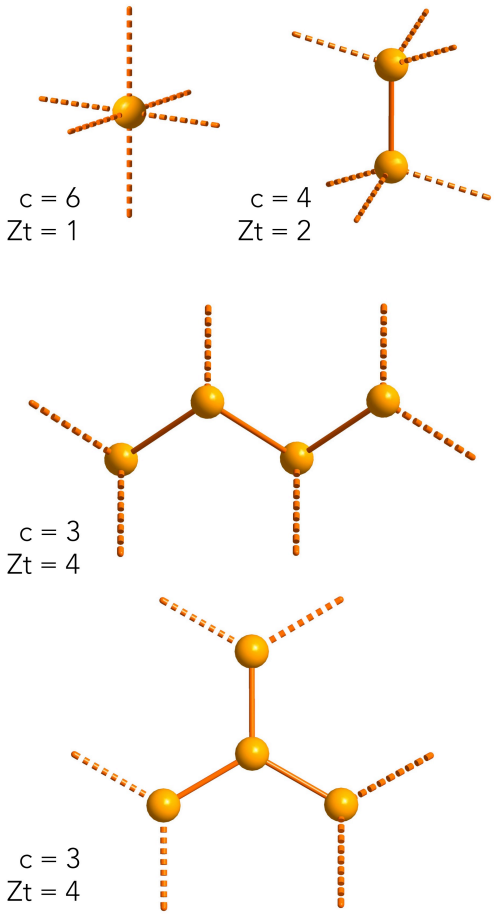

Figure 22 . The minimal repeating units for six-, four- and three-connected nets and the corresponding Z_t numbers.

As shown in Figure 22 there are two ways to establish six connections with a four nodes basic unit. The first one is to have two connections at the extremities and one connection on the two central nodes. The other one is to have two connections at three extremities and none on the central node. These two different arrangements lead to networks 10.3a and 10.3b in the Wells nomenclature or srs and ths in the RCSR (Reticular Chemistry Structure Resource) that are depicted in Figure 23.

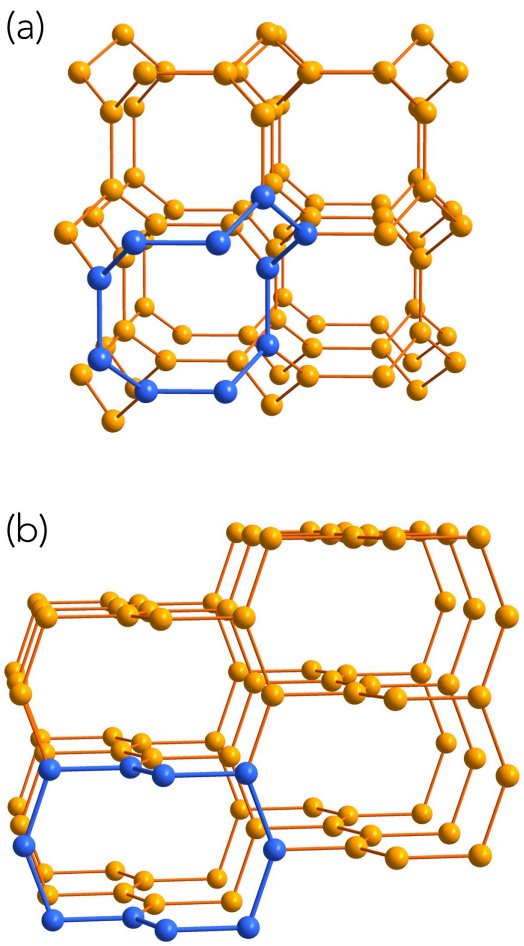

Figure 23. Structure of the ideal (a) 10.3a (srs) and (b) 10.3b (ths) networks.

Starting from this analysis, how is it possible to obtain these networks using dianionic mononuclear copper(II) complexes $[Cu^{II}L_x]^{2-}$ as bis-bidentate metalloligands toward fully solvated metal ions? The main difference between these two networks is the chirality of the 10.3a one and this property gives the lever to generate this network from bis-bidentate metalloligands. As described in the above paragraph for the 2D networks, the honeycomb structure is obtained for a perfect alternation of the chirality of the tris-chelated metal ions. Consequently, a compound where all the tris-chelated metal ions have the same chirality Δ or Λ will adopt the 10.3a network. In order to reach this target, two possible strategies are possible. The first one is to introduce a chiral group in the oxamate ligand and use an enantiopure ligand hoping that it will transfer its chirality to the tris-chelated metal ion to form $\{Cat_2[M_2(Cu^{II}L_x)_3]\}_n$. The groups in València and in Paris tried this approach with the $[Cu\{(M)\text{-binaba}\}]^{2-}$ and $[Cu\{(P)\text{-binaba}\}]^{2-}$ mononuclear complex but up to now they were unable to obtain $[Cat_2\{M_2[Cu\{(M)\text{-binaba}\}]_n$ or $[Cat_2\{M_2[Cu\{(P)\text{-binaba}\}]_n$ 3D network.

The other possibility is to introduce the chirality on the counter cation. This effect was observed in $[Cat\{M_2[M'(ox)_3]_3\}]_n$ where the 10.3a anionic network was induced by the

tris-chelated $[ML_3]^{2+}$ complexes.[81–84] which perfectly fit the cavity size and shape of the 10.3a network. Within the oxamato network, the size of the expected cavity are much larger. The metal-metal distance between the two chiral octahedra are ca. 10.6 Å in the oxamato network and only 5 Å in the oxalato net. Consequently, the $[M(bipy)_3]^{2+}$ or $[M(phen)_3]^{2+}$ entities would not fit the cavity size for a network built with the oxamate ligand. Instead of the $[ML_3]^{2+}$ complex, the enantiopure quaternary ammonium cations (*S*)-trimethyl-(1-phenylethyl)ammonium was used as chiral inducer. By reacting [(*S*)-(1-PhEt)-$Me_3N]_2[Cu^{II}(Et_2pma)_2]\cdot 4H_2O$ with $MnCl_2$, $\{[(S)$-(1-PhEt)$Me_3N]_4[Mn_4Cu_6(Et_2pma)_{12}](DMSO)_3]\cdot 3DMSO\cdot 5H_2O\}_n$ (**3D-MnCu-Et$_2$pma-a**)) was synthesized and the 10.3a (srs) net was obtained as expected, but interestingly, two interpenetrated anionic 3D networks of opposite chirality, (Δ)-$Mn^{II}_2Cu^{II}_3$ and (Λ)-$Mn^{II}_2Cu^{II}_3$, coexist in the structure together with (*S*)-(1- PhEt)Me_3N^+ cations and free H_2O and DMSO molecules. (see Figures 24 and 25)[85]

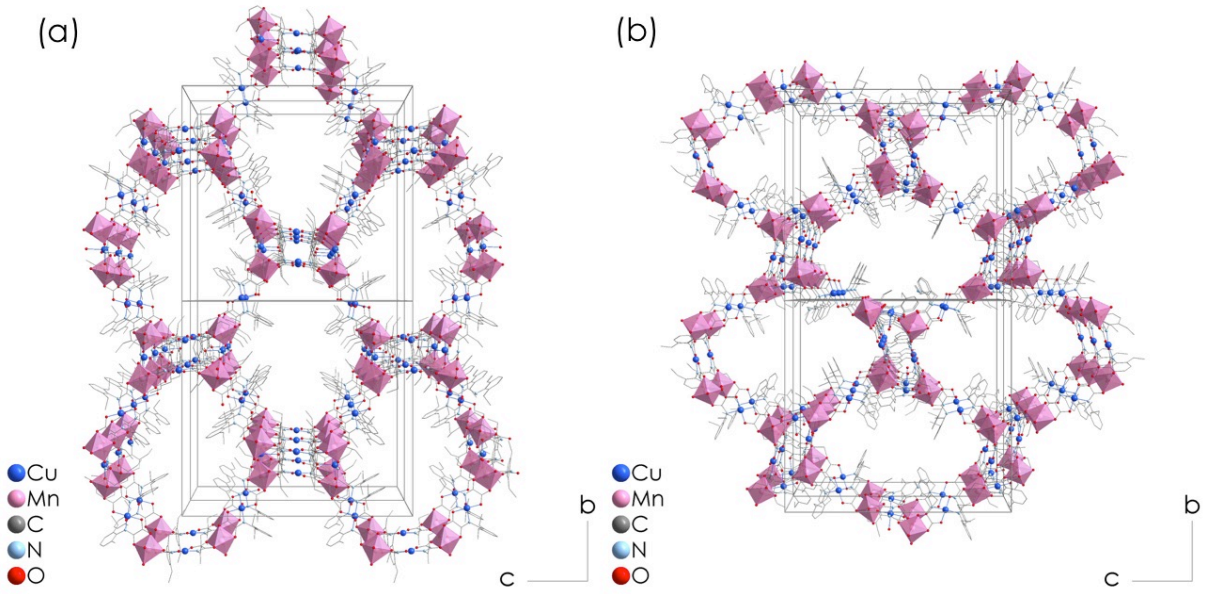

Figure 24. Perspective views of the two interpenetrated networks of $\{[Mn_4Cu_6(Et_2pma)_{12}](DMSO)_3]\}_n^{4n-}$.

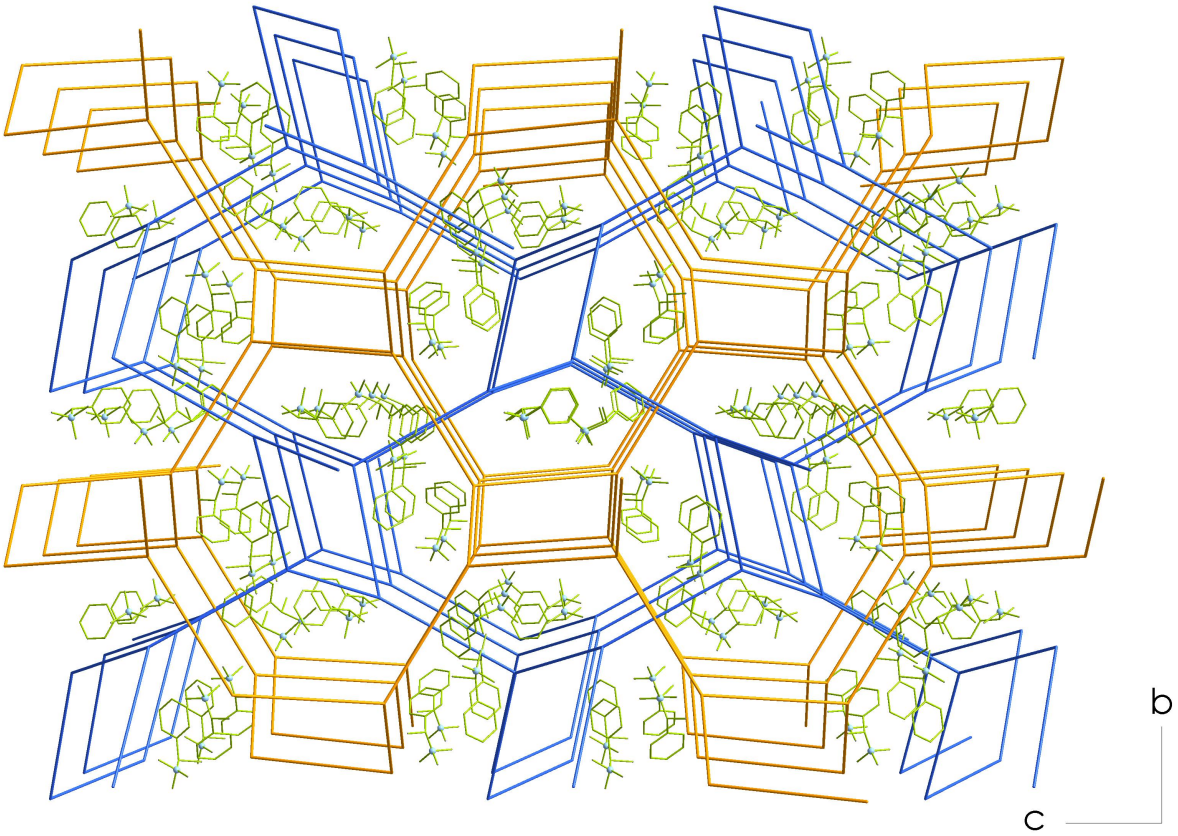

Figure 25. Perspective view of the doubly interpenetrated 3D framework of **3D-MnCu-Et$_2$pma-a** along the [100] direction showing the (*S*)-(1- PhEt)Me$_3$N cations.

As expected for 3D networks, **3D-MnCu-Et2pma-a** presents a magnetic ordering at 15 K (see Figure 26). However, the ordering temperature is relatively low when compared to oxamate-based 2D networks. This is probably due to the observed distortion of the four- and five-coordinate copper(II) ions. The values of the tetrahedricity parameter (δ) at the four-coordinate CuII ions are in the range of 13.7–19.0° (δ = 0 and 90° for the ideal square plane and tetrahedron, respectively), while those of the trigonality parameter (τ) at the five-coordinate square-pyramidal CuII ions are in the range of 0.21–0.26 (τ = 0 and 1 for the ideal square and trigonal bipyramid, respectively)[85].

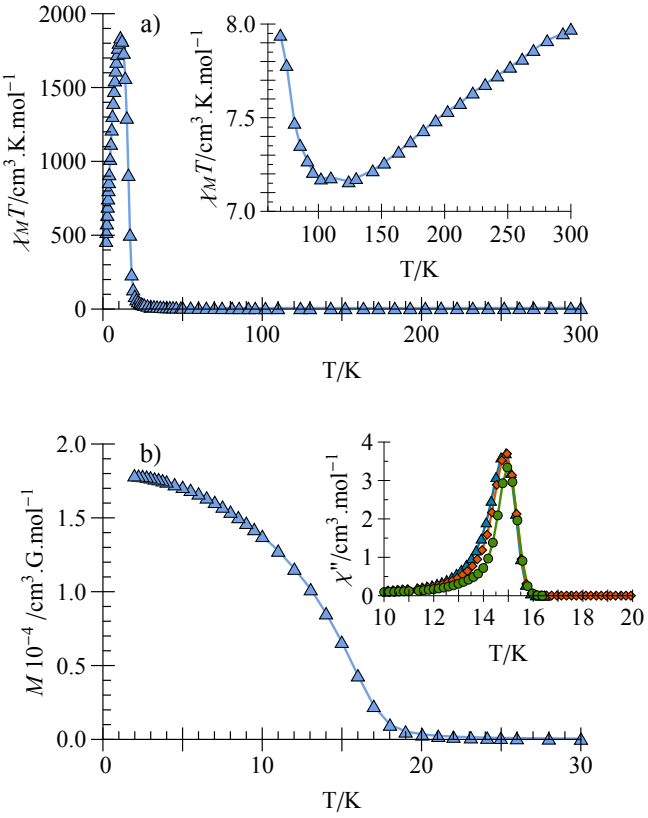

Figure 26. (a) Temperature dependence of $\chi_M T$ for **3D-MnCu-Et2pma-a** under an applied dc field of 0.1 kG (T < 50 K) and 10 kG (T ≥ 50 K). The inset shows the minima in detail. (b) FCM for **3D-MnCu-Et2pma-a**, measured upon cooling within a field of 100 G. The inset shows the temperature dependence of χ_M'' with a 1.0 G oscillating field at different frequencies: 100 Hz (blue), 2.1 kHz (orange), and 10 kHz (green). The solid lines are only eye guides.

If it is possible to benefit from the lever of chirality to induce the 3D 10.3a network and it seems difficult to find a mean to induce the 10.3b one. Unexpectedly, with the use of same Et_2pma ligand by reacting (n-$Bu_4N)_2[Cu(Et_2pma)_2]\cdot 2H_2O$ with $Mn(NO_3)_2\cdot 4H_2O$ $(n\text{-}Bu_4N)_4[Mn_4Cu_6(Et_2pma)_{12}]DMSO\ 10H_2O$ (**3D-MnCu-Et2pma-b**) was synthesized. The classical 6^3-hcb honeycomb network is not obtained but instead a 3D 10.3b ths net is observed. The structure can be described as an extended parallel array of oxamato-bridged manganese(II)–copper(II) chains running along the [10-1] direction with a ΔΔΛΛ sequence for the chirality of the manganese(II) ions (Figure 27).

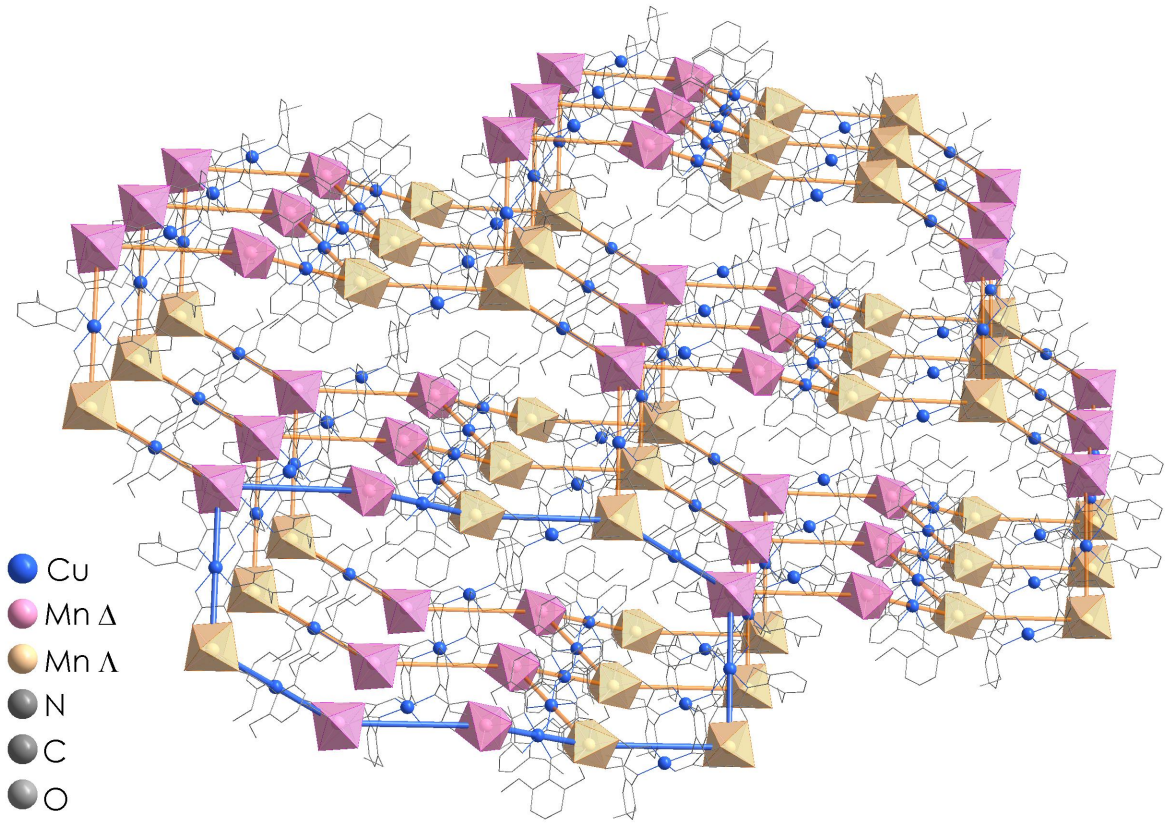

Figure 27. Perspective view of the anionic 2D network of $[Mn_4Cu_6(Et_2pma)_{12}]^{4-}$ along the [111] direction.

It is interesting to compare the magnetic properties of **3D-MnCu-Et2pma-b** with those of **2D-MnCu-Me$_2$pma** which has a 2D 6^3-hcb honeycomb structure. The magnetic properties of both compounds have been modeled by Quantum Monte Carlo calculations (QMC). The best fit of the experimental data gives almost the same value for the exchange interaction between the copper(II) and manganese(II) ions with J_{CuMn}= -35.1 cm^{-1} and -36.1 cm^{-1} for **2D-MnCu-Me$_2$pma** and **3D-MnCu-Et2pma-b** respectively. The connectivity of the networks are identical with three and two neighbors for the Mn(II) and Cu(II) ions, respectively. However, as depicted in Figure 28, the magnetic properties are drastically different with a magnetic ordering at 20 K for the 3D networks and only 10 K for the 2D one and this is only due to the respective dimensionality of the networks.

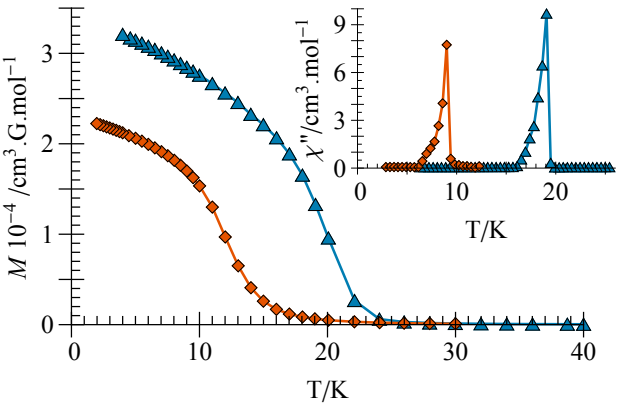

Figure 28. dc field of 100 G for **2D-MnCu-Me$_2$pma** (orange losange) and **3D-MnCu-Et2pma-b** (blue triangle). The field-cooled magnetization (FCM) was measured upon cooling within the field. The inset shows the temperature dependence of the out-of-phase susceptibility for **2D-MnCu-Me$_2$pma** (orange losange) and **3D-MnCu-Et2pma-b** (blue triangle) with a 1.0 G oscillating field at a frequency of 1000 Hz. The solid lines are eye-guides.

For a network build from isotropic Mn(II) ions and weakly anisotropic Cu(II) ions an Heisenberg behavior is expected until the very low temperature and as shown in Table 1 there is no magnetic ordering in that case for a 2D network. So the magnetic ordering for **2D-MnCu-Me$_2$pma** is obtained by the small interplane interaction that explains the lower value of the ordering temperature for the 2D networks and show the importance of obtaining 3D networks by design to get MBMs.

As discussed in the part devoted to the 2D networks, it is possible to increase the dimensionality of the CPs by using dinuclear complexes as starting bricks, the organic parts of the dinuclear complex acting as linker between the heterometallic chains. In the same way it is possible to link the 2D network by pillars made of the organic parts of the dinuclear complex. However, these pillars have to fulfill one requirement. In order to be able to coordinate the octahedral metal ions, the bidentate oxamate group must have an approach angle close to 35.3°. The approach angle as been defined by Raymond as the angle between the vector connecting the two coordinating atoms of a bidentate ligand and the major symmetry axis of the metal center[86,87]. This implies that pillars are not vertical but have to be bent by 35.3° from the perpendicular axis to the plane or that its extremities are bent as shown in Figure 29.

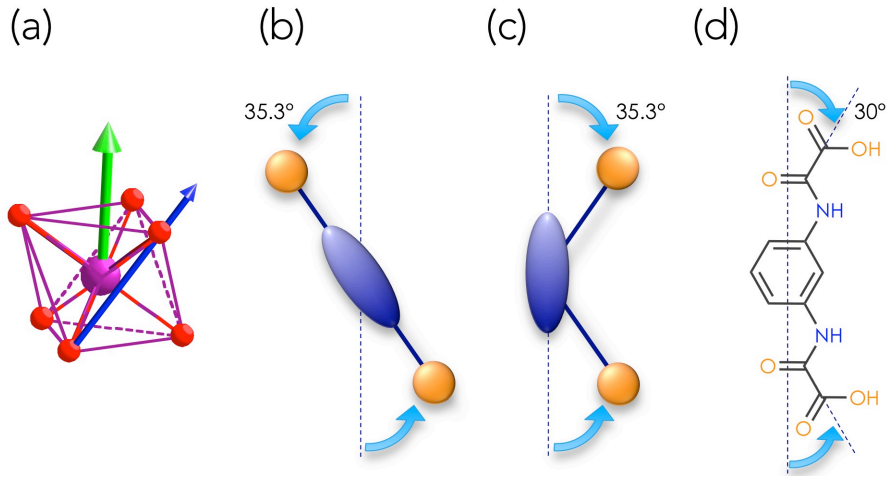

Figure 29. (a) The approach angle is the angle between the blue and green vectors. (b) and (c) Ideal orientation of the bidentate coordination groups in the pillar. (d) Approach angle for the mpba ligands.

In the case of linear pillar (b) the chirality of the two octahedral metal ions are identical. By contrast in case (c) the two octahedral metal ions have opposite chirality. The mpba and substituted mpba ligands present a potential approach angle close to the ideal value of 35.3° which make them very interesting pillars for developing 3D networks. Furthermore the potential approach angles are kept in the dicopper(II) complexes obtained with this family of ligands. Furthermore as shown in the paragraph devoted to the 2D CPs the family of mpba ligands are very efficient FCUs that will lead to ferromagnetic coupling between the 2D layers that is needed to obtain MBMs.

Compounds $[Na(H_2O)_4]_4[Mn_4\{Cu_2(mpba)_2(H_2O)_4\}_3]\cdot 56.5H_2O$ (**H_2O@3D-MnCu-mpba**)[88] and $[Na(H_2O)_{3.25}]_4\{Mn_4[Cu_2(Me3mpba)_2(H_2O)_{3.33}]_3\}\ 37H_2O$ (**H_2O@3D-MnCu-Me_3mpba**)[89] were obtained as bright green tiny crystals by slow diffusion of aqueous solutions of $Na_4[Cu_2(R_3mpba)_2]\cdot x\,H_2O$ (R = H and Me) and $Mn(NO_3)_2\cdot 4H_2O$ (3:4 molar ratio) in an H-shaped tube at room temperature.

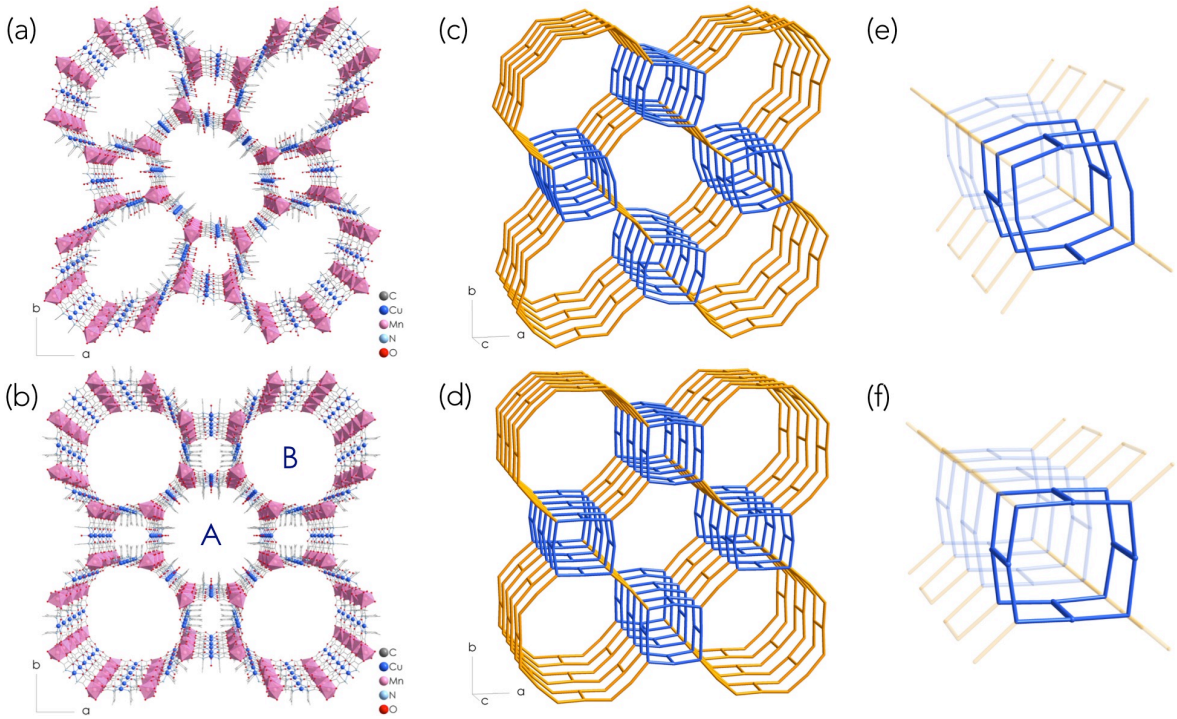

Figure 30. (a, b) Perspective view along the crystallographic c axis of the anionic 3D network for **H_2O@3D-MnCu-mpba** and **H_2O@3D-MnCu-Me_3mpba** respectively (c, d) Schematic view of the 3D networks formed by the metallic centers for **H_2O@3D-MnCu-mpba** and **H_2O@3D-MnCu-Me_3mpba** respectively (e, f) detailed views of the configuration of the pillars linking the 4.8^2 2D networks along the square channels in **H_2O@3D-MnCu-mpba** and **H_2O@3D-MnCu-Me_3mpba** respectively.

As expected, the CPs adopts a 3D structure. However, the layers connected by the pillars do not adopt a honeycomb arrangement but a semi-regular tiling made of octagons and squares (4.8^2 type network)(Figure 30a,b and d,e). These layers are connected by $[Cu_2(R_3mpba)_2]^{4-}$ pillars but two different arrangements are obtained. For **H_2O@3D-MnCu-mpba** there is a regular alternation of upward and downward pillars along the square channels (Figure 30c) with all the phenylene spacers located outward the square. This arrangement leads to non regular alternation of upward and downward pillars around the octagons. Within one layer, half of the octagons have six upward pillars and two downward pillars and the other half present the reverse configuration. Overall this configuration leads to a regular stacking of the 2D 4.8^2 network. For **H_2O@3D-MnCu-Me_3mpba** all the pillars around a square have the same orientation upward or downward (Figure 30f) but with regular alternation of inward and outward orientation for the phenylene spacers. The pillars linking the layer in the opposite direction are located on the edges of the octagon that are not shared with the squares. For these pillars, the orientation of the phenylene spacers is the same than that of the two adjacent squares. These arrangements have two consequences. First, the configuration of the phenylene spacers creates two types of octagonal channels: one hydrophobic containing all the phenylene spacers (A) and the other hydrophilic (B) without inward phenylene. This situation is reflected by their relative diameters of 1.5 (A) and 2.2 nm

(B). Second, the configuration of the pillars creates a dissymmetric stacking of the 4.8^2 planes. Each layer is connected to its neighbors on one side by the pillars located on the square edges and on the other side by the pillars located on the edges shared by two octagons.

H_2O@3D-MnCu-mpba looses easily its water molecules content. The anhydrous phase **3D-MnCu-mpba** is amorphous but the dehydration-hydratation process is reversible and the compound regains its crystallinity (**H_2O@3D-MnCu-mpba'**) (Figure 31a). This reversible process is associated with a large volume change (Figure 31a) and a dramatic modification of the magnetic properties. **H_2O@3D-MnCu-mpba** presents a magnetic ordering at 22.5K, while for the anhydrous **3D-MnCu-mpba** phase the critical temperature is only is only found at Tc = 2.3K (Figure 31b).

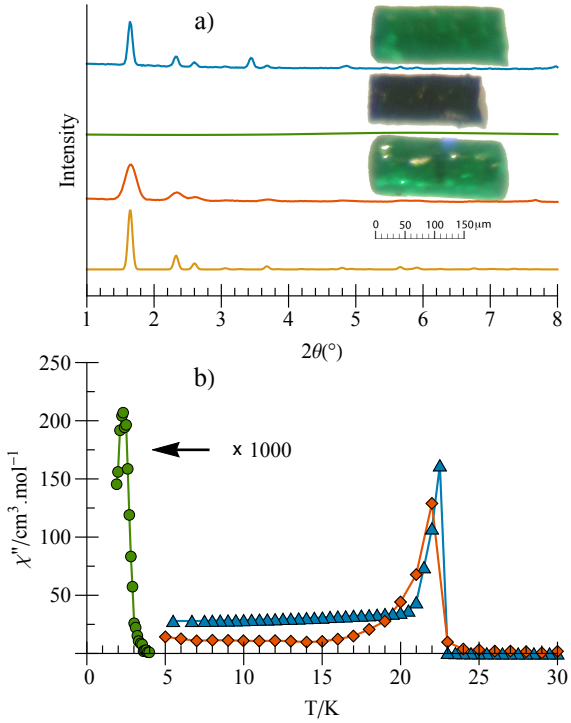

Figure 31. a) XRPD patterns of **H_2O@3D-MnCu-mpba** (blue), **3D-MnCu-mpba** (green), and **H_2O@3D-MnCu-mpba'** (orange) at 25.8°C along with the corresponding single-crystal optical microscopy images. The yellow line corresponds to the calculated XRPD pattern of **H_2O@3D-MnCu-mpba** b)Temperature dependence of χ_M" for **H_2O@3D-MnCu-mpba** (blue triangle), **3D-MnCu-mpba** (green circle), and **H_2O@3D-MnCu-mpba'** (orange losange) with a 4.0 Oe field oscillating at a frequency of 1000 Hz. The peak of χ " for **3D-MnCu-mpba** is shown at 103 amplification. The solid lines are eye-guides.

The amorphous anhydrous phase **3D-MnCu-mpba** shows no porosity and can not uptake others molecules than water thereby suggesting a collapse of the pores in **H_2O@3D-MnCu-mpba** upon deshydratation.

The anhydrous phase **3D-MnCu-Me_3mpba** of **H_2O@3D-MnCu-Me_3mpba** is also amorphous. However for **3D-MnCu-Me_3mpba** the vapor adsorption/ desorption isotherms showed a considerable adsorption of water (17.1 mol kg^{-1}) or methanol

(10.4 mol kg^{-1}) and moderate absorption of CO_2 (3.46 and CH_4(0.95 mol kg^{-1}) (see Figure 32) indicating some porosity of the anhydrous compound **3D-MnCu-Me$_3$mpba** .

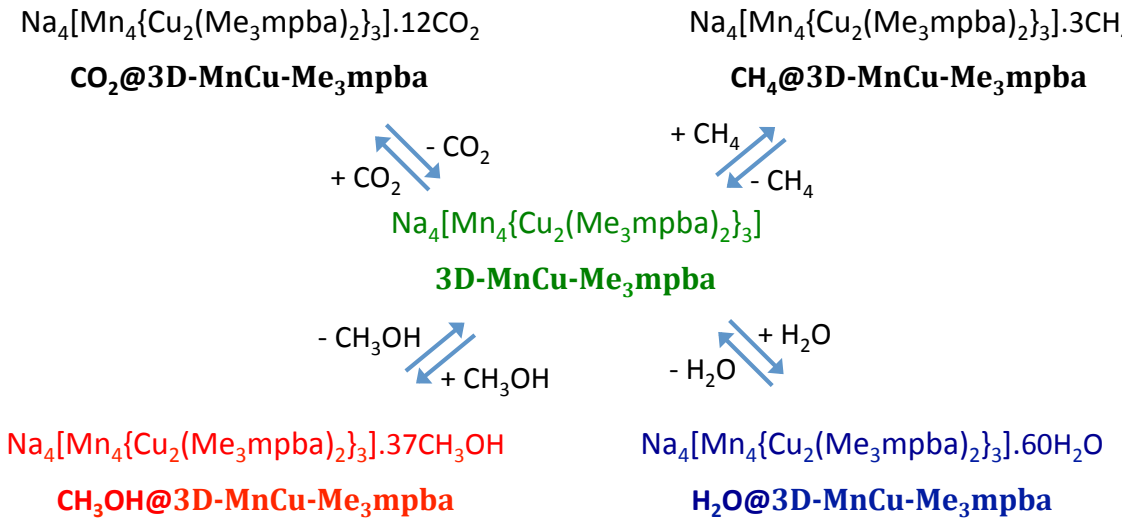

Figure 32. Synthetic route to the different adsorbates of **3D-MnCu-Me$_3$mpba**.

Except for **CO$_2$@3D-MnCu-Me$_3$mpba** and **CH$_4$@3D-MnCu-Me$_3$mpba** the adsorption/ desorption is associated with a dramatic change of the magnetic properties. The trend in the 3D magnetic ordering *Tc* values is *Tc* **3D-MnCu-Me3mpba** ≈ *Tc* **CO2@3D-MnCu-Me3mpba** ≈ *Tc* **CH4@3D-MnCu-Me3mpba** ≈ 2K< *Tc* **CH3OH@3D-MnCu-Me3mpba** =6.5K < *Tc* **H2O@3D-MnCu-Me3mpba** = 21 K as evidenced by the frequency-independent maximum in the χ''M versus T plots (Figure 33). This solvent-dependence of the long-range magnetic ordering temperature in these family of porous magnets offers fascinating possibilities for the magnetic sensing of small guest molecules.

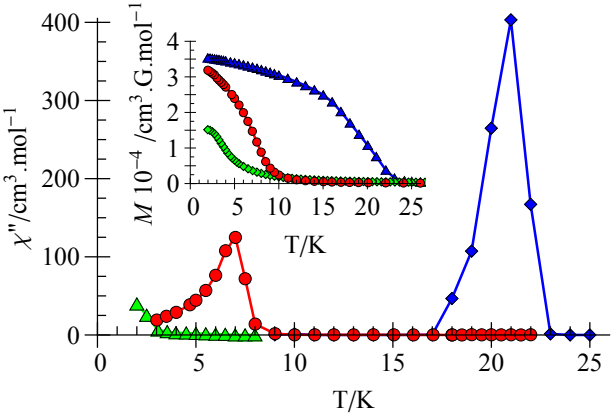

Figure 33. Temperature dependence of the out-of-phase molar ac magnetic susceptibility (χ''_M) of **3D-MnCu-Me3mpba** (green), **CH$_3$OH@3D-MnCu-Me3mpba** (red), and **H$_2$O@3D-MnCu-Me3mpba** (blue) with a ±4.0 G field oscillating at 1000 Hz. The inset shows the temperature dependence of the magnetization (*M*) of the three adsorbates.

The **H$_2$O@3D-MnCu-Me3mpba** compound also presents a remarkable cation exchange properties in the solid-state. One of the sodium counter-ion can be replaced in a single-

crytal to single-crystal process (SC to SC), either by an Fe(III) spin-crossover complex, $[Fe^{III}(sal_2\text{-trien})]NO_3\ H_2O$ (H_2sal_2-trien= N,N^0-disalicylidene- triethylenetetramine)[90] or or by a Mn(III) porphyrin complex, $[MnIII(TPP)(H_2O)_2]ClO_4$ (TPP = 5,10,15,20-tetraphenylporphyrin)[91] to afford $[Fe^{III}(sal_2\text{-trien})]Na_3\{Mn_4[Cu_2(Me_3mpba)_2]_3\}\ 43H_2O$ **$[Fe^{III}(sal_2\text{-trien})]$⊂3D-MnCu-Me$_3$mpba** and $[Mn^{III}(TPP)]Na_3\{Mn_4[Cu_2(Me_3mpba)_2]_3\}\cdot 39\ H_2O$ **$[Mn^{III}(TPP)]$⊂3D-MnCu-Me$_3$mpba** respectively. For **$[Fe^{III}(sal_2\text{-trien})]$⊂3D-MnCu-Me$_3$mpba** the spin conversion 5/2 <-> 1/2 is detectable in the $\chi_M.T$ versus T curve with a sharp decrease of the $\chi_M.T$ value in the 250 K -200 K temperature range. The crystal structure of **$[Mn^{III}(TPP)]$⊂3D-MnCu-Me$_3$mpba** as been solved and is depicted in Figure 34. The $[Mn^{III}(TPP)]^+$ cations occupy the hydrophilic and the hydrophobic octagonal channels.

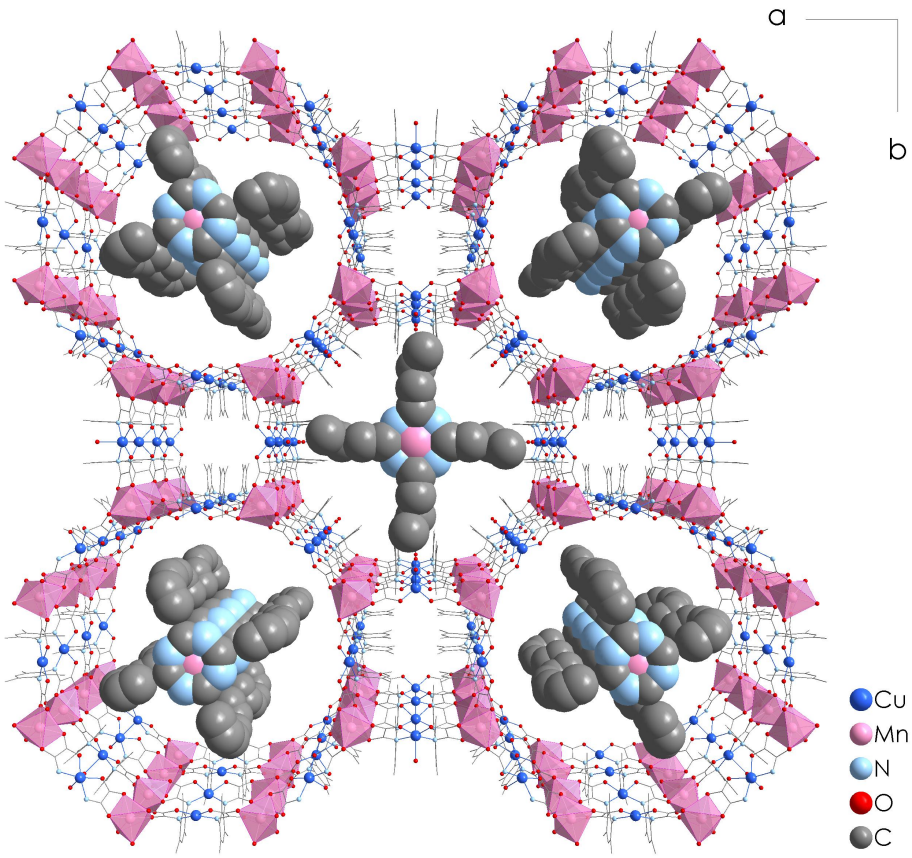

Figure 34. Perspective views along the crystallographic c axis of the hydrophilic (B) and hydrophobic (A) octagonal pores of the hybrid material **$[Mn^{III}(TPP)]$⊂3D-MnCu-Me$_3$mpba** filled by cationic $[Mn^{III}(TPP)(H_2O)_2]+$ complexes

Astonishingly, it is possible not only to exchange the counter cations but also the cations of the network by a SC to SC process. Immersion of crystals of Mg^{II} $\{Mg^{II}[Cu^{II}(Me_3mpba)_2]_3\}\cdot 45H_2O$ (**3D-MgCu-Me$_3$mpba**) in saturated aqueous solutions of $M^{II}(NO_3)_2\cdot 6\ H_2O$ (M^{II} = Co^{II} , Ni^{II}) for several weeks affords new compounds of formulas Co^{II} $\{Co^{II}[Cu^{II}(Me_3mpba)_2]_3\}\cdot 56H_2O$ (**Co⊂3D-CoCu-Me$_3$mpba**) and Ni^{II} $\{Ni^{II}[Cu^{II}(Me_3mpba)_2]_3\}\cdot 54H_2O$.((**Ni⊂3D-NiCu-Me$_3$mpba**))[92] The crystal structures of

all three compounds have been solved and show the same topology than the previous compounds with an extended parallel array of oxamato-bridged $M^{II}_4Cu^{II}_6$ layers growing in the ab plane with a mixed square/octagonal ($4{\cdot}8^2$) net topology. As expected, the Co and Ni compounds presents 3D magnetic ordering at *Tc* = 22 K and 25 K respectively.

In the same spirit, Pardo *et al* have also tried to use mesocate complexes $[M^{II}_2(mpba)_3]^{8-}$ (M^{II}= Ni^{II} and Co^{II}) as pillars between layers, and the $Li_2[Mn_3M_2(mpba)_3(H_2O)_6].22H_2O$ (**3D-MnM-mpba**) (M=Co and Ni) compounds have been prepared[93,94]. The crystal structures are not known but are likely hexagonal 6.3 networks linked by the $[M^{II}_2(mpba)_3]^{8-}$mesocates complexes. However, the exchange interaction in the Co and Ni mesocates is only weakly ferromagnetic and these complexes are therefore poor FCUs leading to 3D magnetic ordering at low temperature only (*Tc*=6.5 K for both compounds).

To conclude this part on 3D CPs, bis-bidentate oxamate ligands or poly bis-bidentate oxamate ligands both allow the synthesis of 3D CPs using different strategies. The most exciting results are obtained with double-stranded dicopper(II) metallacyclophane precursor complexes $[Cu_2(L)_2]^{4-}$ that lead to 3D networks with large octagonal channels. Moreover, this family of porous MBMs possesses remarkable chemical and physico-chemical properties, opening up prospects in magnetic sensing or catalysis.

Conclusion

In this review, the elaboration of coordination polymers using oxamate ligands has been outlined. The ligand design and the synthetic strategy have allowed a control of not only the dimensionality of the CPs but also a control of their magnetic properties, either by controlling the interpolymer interaction or by elaborating efficient FCUs and ACUs (see Table S1). A large part of these results rely on the possibility to change the substituent on the nitrogen atom of the amide function allowing a tuning of the steric effects or providing a way to introduce additional properties. As a matter of fact, this strategy has provided 1D polymers that are among the first examples of Single Chain Magnets (SCM) and, as far as we know, the first example of chiral SCM. It has also yielded many Molecule-Based Magnets (MBM) and more recently porous MBM with large octagonal channels. The Spanish, French and Brazilian groups are now expanding their work to the synthesis of multifunctional magnetic materials displaying unique magnetic properties as well as redox, optical, transport, sensing, or catalytic activities. Taking advantage of the chemical flexibility of the oxamate ligands, this kind of materials will probably be easier to obtain with oxamate ligands than with oxalates[95–99]. A special focus will be made on the **3D-MCu-$R_x$mpba** family that presents outstanding chemical properties with the possibility of making post-synthetic transformation in the solid state.

[1] J. S. Miller, J. C. Calabrese, A. J. Epstein, R. W. Bigelow, J. H. Zhang, W. M. Reiff, *J. Chem. Soc. Chem. Commun.* **1986**, 1026–1028.
[2] Y. Pei, M. Verdaguer, O. Kahn, J. Sletten, J. P. Renard, *J. Am. Chem. Soc.* **1986**, *108*, 7428–7430.
[3] A. Caneschi, D. Gatteschi, J. Laugier, P. Rey, *J. Am. Chem. Soc.* **1987**, *109*, 2191–2192.
[4] A. Caneschi, D. Gatteschi, N. Lalioti, C. Sangregorio, R. Sessoli, G. Venturi, A. Vindigni, A. Rettori, M. G. Pini, M. A. Novak, *Angew. Chem. Int. Ed.* **2001**, *40*, 1760–1763.
[5] F. Palacio, in *Magn. Mol. Mater.*, D. Gatteschi, O. Kahn, J. Miller, F. Palacio, Dordrecht Boston London, **1991**, pp. 1–34.
[6] J. M. Kosterlitz, D. J. Thouless, *J. Phys. C Solid State Phys.* **1973**, *6*, 1181.
[7] E. Ising, *Z Phys.* **1925**, *31*, 253.
[8] L. Onsager, *Phys. Rev.* **1944**, *65*, 117.
[9] S. Istrail, in *32nd ACM Symp. Theory Comput.*, ACM Press, **2000**, pp. 87–96.
[10] R. J. Glauber, *J. Math. Phys.* **1963**, 294–307.
[11] A. Caneschi, D. Gatteschi, N. Lalioti, C. Sangregorio, R. Sessoli, G. Venturi, A. Vindigni, A. Rettori, M. G. Pini, M. A. Novak, *Europhys. Lett.* **2002**, *58*, 771–777.
[12] P. W. Anderson, *Phys. Rev.* **1959**, *115*, 2–13.
[13] J. Kanamori, *J. Phys. Chem. Solids* **1959**, *10*, 87–98.
[14] J. B. Goodenough, *Phys. Rev.* **1955**, *100*, 564.
[15] J. B. Goodenough, *Magnetism and the Chemical Bonding*, **1963**.
[16] H. Weihe, H. U. Güdel, H. Toftlund, *Inorg. Chem.* **2000**, *39*, 1351–1362.
[17] O. Kahn, B. Briat, *J. Chem. Soc.-Faraday Trans. Ii* **1976**, *72*, 268–281.
[18] O. Kahn, B. Briat, *J. Chem. Soc.-Faraday Trans. Ii* **1976**, *72*, 1441–1446.
[19] J. J. Girerd, Y. Journaux, O. Kahn, *Chem. Phys. Lett.* **1981**, *82*, 534–538.
[20] P. J. Hay, J. C. Thibeault, R. Hoffmann, *J. Am. Chem. Soc.* **1975**, *97*, 4884–4899.
[21] P. W. Anderson, in *Magnetism*, Academic Press, **1963**.
[22] V. H. Crawford, H. W. Richardson, J. R. Wasson, D. J. Hodgson, W. E. Hatfield, *Inorg. Chem.* **1976**, *15*, 2107–2110.
[23] O. Kahn, J. Galy, Y. Journaux, J. Jaud, I. Morgenstern-Badarau, *J. Am. Chem. Soc.* **1982**, *104*, 2165–2176.
[24] Y. Journaux, O. Kahn, J. Zarembowitch, J. Galy, J. Jaud, *J. Am. Chem. Soc.* **1983**, *105*, 7585–7591.
[25] O. Kahn, *Molecular Magnetism*, VCH Publishers Inc, New York, **1993**.
[26] M. Julve, M. Verdaguer, A. Gleizes, M. Philoche-Levisalles, O. Kahn, *Inorg. Chem.* **1984**, *23*, 3808–3818.
[27] Y. Journaux, J. Sletten, O. Kahn, *Inorg. Chem.* **1985**, *24*, 4063–4069.
[28] J. J. Girerd, O. Kahn, M. Verdaguer, *Inorg. Chem.* **1980**, *19*, 274–276.
[29] M. Verdaguer, M. Julve, A. Michalowicz, O. Kahn, *Inorg. Chem.* **1983**, *22*, 2624–2629.
[30] A. Gleizes, M. Verdaguer, *J. Am. Chem. Soc.* **1984**, *106*, 3727–3737.
[31] D. Luneau, H. Oshio, H. Okawa, M. Koikawa, S. Kida, *Bull. Chem. Soc. Jpn.* **1990**, *63*, 2212–2217.
[32] J. Cano, A. Rodríguez-Fortea, P. Alemany, S. Alvarez, E. Ruiz, *Chem. – Eur. J.* **2000**, *6*, 327–333.
[33] F. Lloret, R. Ruiz, M. Julve, J. Faus, Y. Journaux, I. Castro, M. Verdaguer, *Chem. Mater.* **1992**, *4*, 1150–1153.
[34] F. Lloret, R. Ruiz, B. Cervera, I. Castro, M. Julve, J. Faus, J. A. Real, F. Sapiña, Y.

Journaux, J. C. Colin, et al., *J. Chem. Soc. Chem. Commun.* **1994**, 2615–2616.
[35] M. Ohba, N. Maruono, H. Okawa, T. Enoki, J.-M. Latour, *J. Am. Chem. Soc.* **1994**, *116*, 11566–11567.
[36] M. Ohba, H. Ōkawa, T. Ito, A. Ohto, *J. Chem. Soc. Chem. Commun.* **1995**, 1545–1546.
[37] H. Miyasaka, N. Matsumoto, H. Ōkawa, N. Re, E. Gallo, C. Floriani, *J. Am. Chem. Soc.* **1996**, *118*, 981–994.
[38] H. Miyasaka, N. Matsumoto, H. Ōkawa, N. Re, E. Gallo, C. Floriani, *Angew. Chem. Int. Ed. Engl.* **1995**, *34*, 1446–1448.
[39] S. Ferlay, T. Mallah, J. Vaissermann, F. Bartolome, P. Veillet, M. Verdaguer, *Chem. Commun.* **1996**, 2481.
[40] V. Gadet, T. Mallah, I. Castro, M. Verdaguer, *J. Am. Chem. Soc.* **1992**, *114*, 9213.
[41] T. Mallah, S. Thiébault, M. Verdaguer, P. Veillet, *Science* **1993**, *262*, 1554.
[42] S. Ferlay, T. Mallah, R. Ouahès, P. Veillet, M. Verdaguer, *Nature* **1995**, *378*, 701–703.
[43] W. R. Entley, G. S. Girolami, *Science* **1995**, *268*, 397–400.
[44] M. Verdaguer, A. Bleuzen, V. Marvaud, J. Vaissermann, M. Seuleiman, C. Desplanches, A. Scuiller, C. Train, R. Garde, G. Gelly, et al., *Coord. Chem. Rev.* **1999**, *190*, 1023–1047.
[45] Y. Pei, Y. Journaux, O. Kahn, *Chem. Commun.* **1986**, 1300–13001.
[46] Y. Journaux, J. Sletten, O. Kahn, *Inorg. Chem.* **1986**, *25*, 439–447.
[47] Y. Pei, Y. Journaux, O. Kahn, *Inorg. Chem.* **1988**, *27*, 399–404.
[48] F. Lloret, Y. Journaux, M. Julve, *Inorg. Chem.* **1990**, *29*, 3967–3972.
[49] Y. Pei, O. Kahn, J. Sletten, *J. Am. Chem. Soc.* **1986**, *108*, 3143–3145.
[50] P. M. Richards, *Phys. Rev. B* **1974**, *10*, 4687–4689.
[51] H. M. McConnell, *J. Chem. Phys.* **1963**, *39*, 1910–1910.
[52] V. Baron, B. Gillon, J. Sletten, C. Mathoniere, E. Codjovi, O. Kahn, *Inorganica Chim. Acta* **1995**, *235*, 69–76.
[53] K. Nakatani, J. Y. Carriat, Y. Journaux, O. Kahn, F. LLoret, J. P. Renard, Y. Pei, Y. Sletten, M. Verdaguer, *J. Am. Chem. Soc.* **1989**, *111*, 5739.
[54] F. Lloret, M. Julve, R. Ruiz, Y. Journaux, K. Nakatani, O. Kahn, J. Sletten, *Inorg. Chem.* **1993**, *32*, 27–31.
[55] K. Nakatani, P. Bergerat, E. Codjovi, C. Mathoniere, Y. Pei, O. Kahn, *Inorg. Chem.* **1991**, *30*, 3977–3978.
[56] E. Pardo, R. Ruiz-García, F. Lloret, J. Faus, M. Julve, Y. Journaux, F. Delgado, C. Ruiz-Pérez, *Adv. Mater.* **2004**, *16*, 1597–1600.
[57] E. Pardo, R. Ruiz-García, F. Lloret, J. Faus, M. Julve, Y. Journaux, M. A. Novak, F. S. Delgado, C. Ruiz-Pérez, *Chem. – Eur. J.* **2007**, *13*, 2054–2066.
[58] E. Pardo, C. Train, R. Lescouëzec, Y. Journaux, J. Pasán, C. Ruiz-Pérez, F. S. Delgado, R. Ruiz-Garcia, F. Lloret, C. Paulsen, *Chem. Commun.* **2010**, *46*, 2322–2324.
[59] J. Ferrando-Soria, D. Cangussu, M. Eslava, Y. Journaux, R. Lescouëzec, M. Julve, F. Lloret, J. Pasán, C. Ruiz-Pérez, E. Lhotel, et al., *Chem. – Eur. J.* **2011**, *17*, 12482–12494.
[60] G. L. A. Rikken, E. Raupach, *Nature* **1997**, *390*, 493–494.
[61] C. Train, R. Gheorghe, V. Krstic, L. M. Chamoreau, N. S. Ovanesyan, G. Rikken, M. Gruselle, M. Verdaguer, *Nat. Mater.* **2008**, *7*, 729–734.
[62] Y. Journaux, R. Ruiz, A. Aukauloo, Y. Pei, *Mol. Cryst. Liq. Cryst. Sci. Technol. Sect. Mol. Cryst. Liq. Cryst.* **1997**, *305*, 193–202.
[63] L. Carlucci, G. Ciani, D. M. Proserpio, *Coord. Chem. Rev.* **2003**, *246*, 247–289.
[64] H. O. Stumpf, Y. Pei, O. Kahn, L. Ouahab, D. Grandjean, *Science* **1993**, *261*, 447–449.

[65] M. G. F. Vaz, L. M. M. Pinheiro, H. O. Stumpf, A. F. C. Alcântara, S. Golhen, L. Ouahab, O. Cador, C. Mathonière, O. Kahn, *Chem. – Eur. J.* **1999**, *5*, 1486–1495.
[66] O. Cador, M. G. F. Vaz, H. O. Stumpf, C. Mathonière, O. Kahn, *Synth. Met.* **2001**, *122*, 559–567.
[67] O. Cador, M. G. F. Vaz, H. O. Stumpf, C. Mathonière, *J. Magn. Magn. Mater.* **2001**, *234*, 6–12.
[68] M. G. F. Vaz, H. O. Stumpf, N. L. Speziali, C. Mathonière, O. Cador, *Polyhedron* **2001**, *20*, 1761–1769.
[69] J. Ferrando-Soria, T. Grancha, M. Julve, J. Cano, F. Lloret, Y. Journaux, J. Pasán, C. Ruiz-Pérez, E. Pardo, *Chem. Commun.* **2012**, *48*, 3539–3541.
[70] L. Atovmyan, G. Shilov, R. Lyubovskaya, E. Zhilyaeva, N. Ovanesyan, S. Pirumova, I. Gusakovskaya, Y. Morozov, *Jetp Lett.* **1993**, *58*, 766–769.
[71] S. Decurtins, H. W. Schmalle, H. R. Oswald, A. Linden, J. Ensling, P. Gütlich, A. Hauser, *Inorganica Chim. Acta* **1994**, *216*, 65–73.
[72] P. Karafiloglou, *J. Chem. Educ.* **1989**, *66*, 816.
[73] I. Fernandez, R. Ruiz, J. Faus, M. Julve, F. Lloret, J. Cano, X. Ottenwaelder, Y. Journaux, M. C. Munoz, *Angew. Chem. Int. Ed.* **2001**, *40*, 3039–3042.
[74] E. Pardo, J. Faus, M. Julve, F. Lloret, M. C. Muñoz, J. Cano, X. Ottenwaelder, Y. Journaux, R. Carrasco, G. Blay, et al., *J. Am. Chem. Soc.* **2003**, *125*, 10770–10771.
[75] E. Pardo, R. Ruiz-García, J. Cano, X. Ottenwaelder, R. Lescouëzec, Y. Journaux, F. Lloret, M. Julve, *Dalton Trans.* **2008**, 2780–2805.
[76] C. L. M. Pereira, E. F. Pedroso, H. O. Stumpf, M. A. Novak, L. Ricard, R. Ruiz-García, E. Rivière, Y. Journaux, *Angew. Chem. Int. Ed.* **2004**, *43*, 956–958.
[77] J. Ferrando-Soria, J. Pasán, C. Ruiz-Pérez, Y. Journaux, M. Julve, F. Lloret, J. Cano, E. Pardo, *Inorg. Chem.* **2011**, *50*, 8694–8696.
[78] Y. Filali, Synthesis and physico-chemical studies of one-dimensional magnetic heterometallic compounds, UPMC, **2007**.
[79] H. Heesch, F. Laves, *Z. Für Krist. - Cryst. Mater.* **1933**, *85*, 443–453.
[80] A. F. Wells, *Acta Crystallogr.* **1954**, *7*, 535–544.
[81] S. Decurtins, H. W. Schmalle, P. Schneuwly, *Inorg. Chem.* **1993**, *32*, 1888.
[82] S. Decurtins, H. W. Schmalle, P. Schneuwly, J. Ensling, P. Gütlich, *J. Am. Chem. Soc.* **1994**, *116*, 9521–9528.
[83] S. Decurtins, H. W. Schmalle, R. Pellaux, P. Schneuwly, A. Hausers, *Inorg. Chem.* **1996**, *35*, 1451–1460.
[84] M. Hernández-Molina, F. Lloret, C. Ruiz-Pérez, M. Julve, *Inorg. Chem.* **1998**, *37*, 4131–4135.
[85] T. Grancha, M. Mon, F. Lloret, J. Ferrando-Soria, Y. Journaux, J. Pasán, E. Pardo, *Inorg. Chem.* **2015**, *54*, 8890–8892.
[86] D. L. Caulder, K. N. Raymond, *Acc. Chem. Res.* **1999**, *32*, 975–982.
[87] D. L. Caulder, K. N. Raymond, *J. Chem. Soc. Dalton Trans.* **1999**, 1185–1200.
[88] J. Ferrando-Soria, R. Ruiz-García, J. Cano, S.-E. Stiriba, J. Vallejo, I. Castro, M. Julve, F. Lloret, P. Amorós, J. Pasán, et al., *Chem. Eur. J.* **2012**, *18*, 1608–1617.
[89] J. Ferrando-Soria, P. Serra-Crespo, M. de Lange, J. Gascon, F. Kapteijn, M. Julve, J. Cano, F. Lloret, J. Pasán, C. Ruiz-Pérez, et al., *J. Am. Chem. Soc.* **2012**, *134*, 15301–15304.
[90] A. Abhervé, T. Grancha, J. Ferrando-Soria, M. Clemente-León, E. Coronado, J. C. Waerenborgh, F. Lloret, E. Pardo, *Chem. Commun.* **2016**, *52*, 7360–7363.
[91] M. Mon, A. Pascual-Álvarez, T. Grancha, J. Cano, J. Ferrando-Soria, F. Lloret, J. Gascon, J. Pasán, D. Armentano, E. Pardo, *Chem. – Eur. J.* **2016**, *22*, 539–545.
[92] T. Grancha, J. Ferrando-Soria, H.-C. Zhou, J. Gascon, B. Seoane, J. Pasán, O. Fabelo,

M. Julve, E. Pardo, *Angew. Chem. Int. Ed.* **2015**, 6521–6525.
[93] E. Pardo, D. Cangussu, M.-C. Dul, R. Lescouëzec, P. Herson, Y. Journaux, E. F. Pedroso, C. L. M. Pereira, M. C. Muñoz, R. Ruiz-García, et al., *Angew. Chem. Int. Ed.* **2008**, *47*, 4211–4216.
[94] D. Cangussu, E. Pardo, M.-C. Dul, R. Lescouëzec, P. Herson, Y. Journaux, E. F. Pedroso, C. L. M. Pereira, H. O. Stumpf, M. Carmen Muñoz, et al., *Inorganica Chim. Acta* **2008**, *361*, 3394–3402.
[95] E. Coronado, J. R. Galán-Mascarós, C. J. Gómez-García, V. Laukhin, *Nature* **2000**, *408*, 447–449.
[96] C. Train, T. Nuida, R. Gheorghe, M. Gruselle, S. Ohkoshi, *J. Am. Chem. Soc.* **2009**, *131*, 16838–16843.
[97] E. Pardo, C. Train, G. Gontard, K. Boubekeur, O. Fabelo, H. Liu, B. Dkhil, F. Lloret, K. Nakagawa, H. Tokoro, et al., *J. Am. Chem. Soc.* **2011**, *133*, 15328–15331.
[98] E. Pardo, C. Train, H. Liu, L.-M. Chamoreau, B. Dkhil, K. Boubekeur, F. Lloret, K. Nakatani, H. Tokoro, S. Ohkoshi, et al., *Angew. Chem. Int. Ed.* **2012**, *51*, 8356–8360.
[99] C. Maxim, S. Ferlay, H. Tokoro, S.-I. Ohkoshi, C. Train, *Chem. Commun.* **2014**, *50*, 5629–5632.